AD 291 765

DISCLAIMER NOTICE

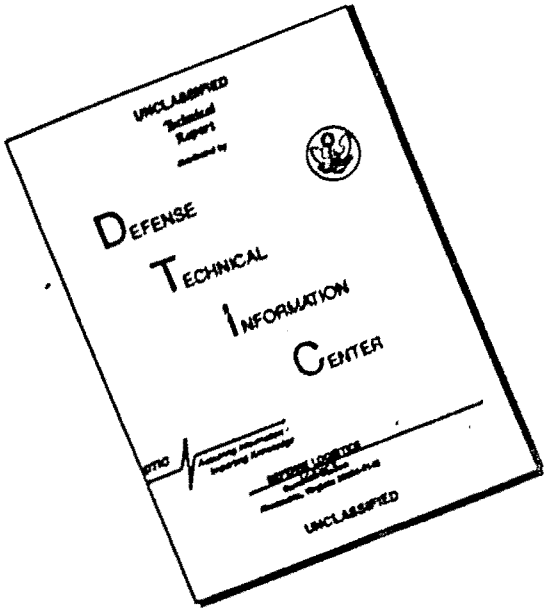

THIS DOCUMENT IS BEST QUALITY AVAILABLE. THE COPY FURNISHED TO DTIC CONTAINED A SIGNIFICANT NUMBER OF PAGES WHICH DO NOT REPRODUCE LEGIBLY.

53-1-6

ANTENNA LABORATORY

Technical Report No. 60

BACKWARD-WAVE RADIATION FROM PERIODIC STRUCTURES AND APPLICATION TO THE DESIGN OF FREQUENCY-INDEPENDENT ANTENNAS

by

P. E. Mayes

G. A. Deschamps

W. T. Patton

Contract AF33(657)-8460

Hitch Element Nr. 62405454

760D — Project 4028, Task 402824

Aeronautical Systems Division

Project Engineer E. Turner, ASRNCF-1

DECEMBER 1962

Sponsored by:

AERONAUTICAL SYSTEMS DIVISION

WRIGHT-PATTERSON AIR FORCE BASE, OHIO

ELECTRICAL ENGINEERING RESEARCH LABORATORY

ENGINEERING EXPERIMENT STATION

UNIVERSITY OF ILLINOIS

URBANA, ILLINOIS

Antenna Laboratory

Technical Report No. 60

BACKWARD-WAVE RADIATION FROM PERIODIC STRUCTURES AND APPLICATION TO THE DESIGN OF FREQUENCY-INDEPENDENT ANTENNAS

by

P. E. Mayes
G. A. Deschamps
W. T. Patton

Contract AF33(657)-8460
Hitch Element Nr. 62405454
760D - Project 4028, Task 402824
Aeronautical Systems Division
Project Engineer E. Turner, ASRNCF-1

December 1962

Sponsored by:

Aeronautical Systems Division
Wright-Patterson Air Force Base, Ohio

ELECTRICAL ENGINEERING RESEARCH LABORATORY
ENGINEERING EXPERIMENT STATION
UNIVERSITY OF ILLINOIS
URBANA, ILLINOIS

ACKNOWLEDGMENT

Several members of the Antenna Laboratory staff have contributed to the measurements reported herein. The helix-fed monopole experiments and tests of the log-periodic bent zigzag were done by John W. Greiser. Model construction and testing of the zigzag, helix, and dipole array antennas was done by Bradley Martin, Ron Grant, and Eddie Young.

CONTENTS

		Page
1.	Introduction	1
2.	Periodic Structures	2
3.	The Helix-Fed Monopole Array	13
4.	The Bifilar Zig Zag and Helix Antennas	25
5.	Resonant Periodic Structures	43
6.	Conclusions	53
References		55

ILLUSTRATIONS

Figure Number		Page
1.	Diffracted waves produced by a periodic grating	3
2.	A periodic grating imposed on a slow wave transmission system	5
3.	A Brillouin diagram showing a slow wave phase constant	7
4.	Universal pattern chart for exponential current distributions on discrete arrays	10
5.	Radiation patterns typical of exponential taper slow wave current distributions	11
6.	A periodic monopole array with a helical delay line feed	14
7.	Space harmonics for sampling a slow wave at a specific rate	15
8.	Experimental model of a helix-fed monopole array	17
9.	H-plane radiation pattern of a helix-fed monopole array	18
10.	Brillouin diagram for helix-fed monopole arrays	22
11.	A log-periodic helix-fed monopole array	23
12.	Periodic zig zag and helical wire structures	26
13.	A monofilar zig zag wire antenna	28
14.	H-plane radiation patterns of a monofilar zig zag antenna	29
15.	H-plane radiation patterns of a bifilar zig zag antenna as a function of number of cells	31
16a.	H-plane radiation patterns of a bifilar zig zag antenna as a function of frequency	32
16b.	E-plane radiation patterns of a bifilar zig zag antenna as a function of frequency	33
17.	Brillouin diagram for a bifilar zig zag	35
18.	Current amplitude distribution for a bifilar zig zag antenna	36
19.	A log-periodic bifilar zig zag antenna	38

20. Radiation patterns of a log-periodic bifilar zig zag antenna 39

21. A log-periodic monofilar zig zag over ground 40

22. Radiation patterns of a log-periodic monofilar zig zag over ground 41

23. Vertically-polarized log-periodic zig zag antennas over ground 42

24. A periodic array of dipoles 44

25. Feeder voltage versus distance on a periodic dipole array 45

26. Brillouin diagram for feeder voltage on a periodic dipole array 47

27. H-plane radiation patterns of a periodic dipole array 49

28. Transformation of measured Brillouin diagram of feeder voltage along periodic dipole array to diagram showing phasing of dipoles 50

29. Brillouin diagram for dipole currents 52

1. INTRODUCTION

One characteristic common to a large number of unidirectional frequency-independent log-periodic and log-spiral antennas is that radiation is directed toward the apex or feed point of the structure[1,2,3]. This property is essential to the frequency-independent behavior of the finite antenna since it makes less important the end effect due to truncation on the side of the large elements of the structure. That this is so can be seen from the requirement that the total current on the structure must decay with distance from the feed point to avoid a large reflection from the large-end truncation. This in turn requires that the fields along the antenna structure decay more rapidly than inversely with distance. This last condition is met only when the far field pattern vanishes in the direction of the antenna structure.

In attempting to explain this property and more generally to understand the operation of log-periodic antennas it is found useful to think of the antenna as a locally periodic structure whose period varies slowly, increasing linearly with distance from the apex. This report will develop the idea by describing the results obtained experimentally with a number of uniformly periodic antennas. A more rigorous and detailed examination of several of the structures will be contained in subsequent reports.

2 PERIODIC STRUCTURES

Consider first the somewhat idealized problem of the diffraction of a plane wave by an infinite, periodic grating. Let the z-axis lie in the plane of the grating, perpendicular to the lines of the grating as shown in Figure 1. It is well known that a number of diffracted waves are produced. If the incident wave has a propagation vector $\vec{k}$ with a projection β_o on the z-axis, the diffracted wave of order n will have a propagation vector $\vec{k}_n$ with a projection

$$\beta_n = \beta_o - np \qquad n\text{-integer} \tag{1}$$

on the z-axis. In this formula $p = \frac{2\pi}{a}$ where a is the period of the grating. The wave characterized by β_o is the fundamental wave; those described by $\beta_n (n \neq 0)$ are the space harmonics. Only a finite number of the vectors $\vec{k}_n$ are real, those for which

$$|\beta_n| < k = \omega\sqrt{\mu\epsilon} \tag{2}$$

Equation (2) defines the "visible range" of the space spectrum which represents waves propagating obliquely with respect to the grating axis. The length of the propagation vector $\vec{k}_n$ for these oblique waves is equal to the intrinsic phase constant of the medium, k, as shown in Figure 1. For all waves outside the visible range the components of the propagation vectors normal to the surface are imaginary and the waves are evanescent waves traveling along the plane of the grating. For a finite grating the beams produced by the oblique waves are not infinitely sharp. The width of beams nearly broadside to the grating is approximately the inverse of the length of the grating measured in wavelengths. The relative amplitudes of the various beams depend on the detailed form of the lines of the grating.

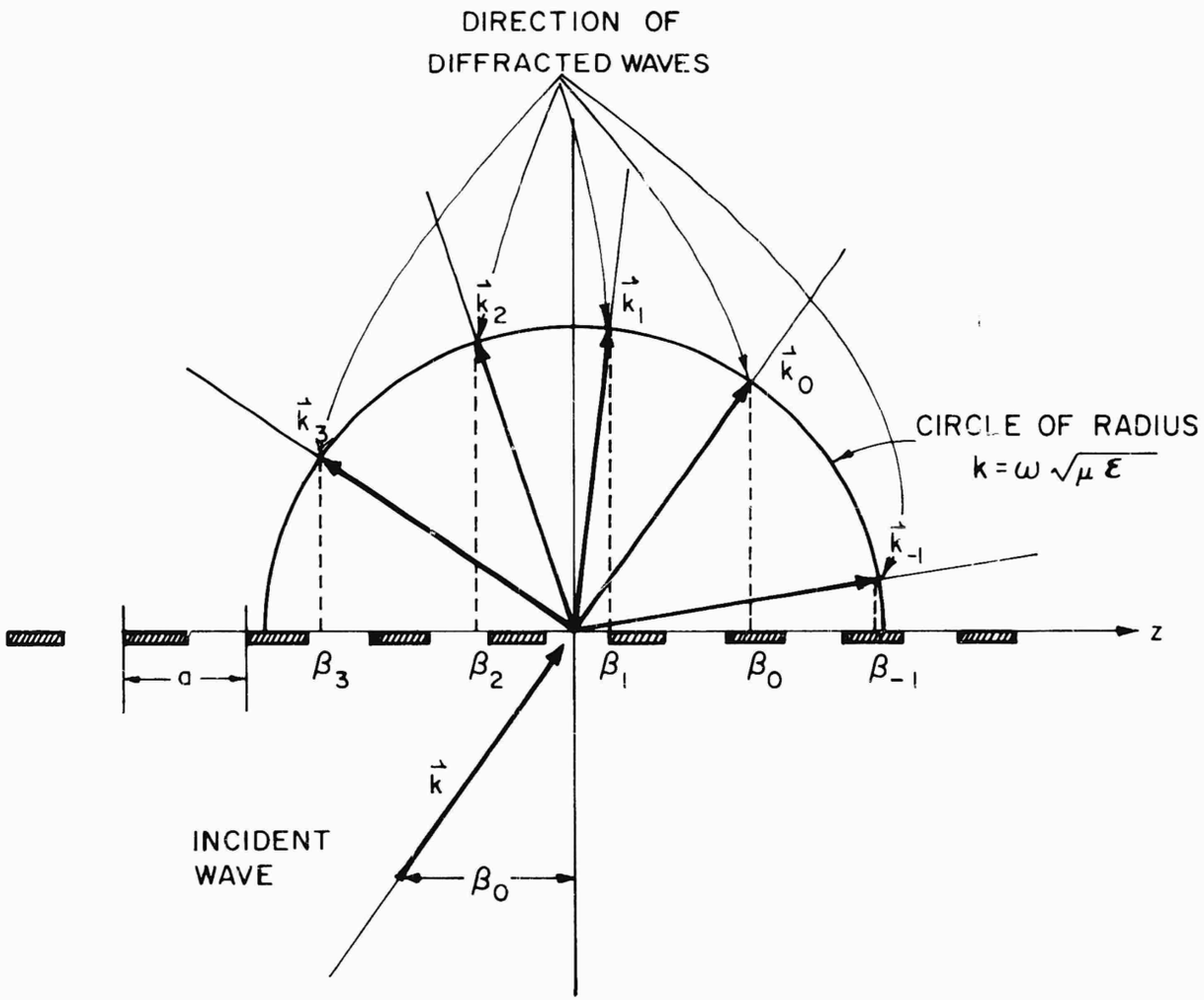

Figure 1. Diffracted waves produced by a periodic grating

The same description applies to the diffraction of an incident wave having a complex propagation vector or to any wave guided along an infinite grating and having a phase constant β_o in that direction. For example, Figure 2 shows a dielectric slab bounded on one side by a conductor and on the other side by a grating. If this supports a slow fundamental wave ($\beta_o > k$) and if the period a is small, p will be large and all the $\beta_n = \beta_o - np$ (for n positive or negative integer) will be larger than k. None of the diffracted waves has a real direction of propagation which means that no oblique wave occurs. If now the spacing is increased, p will become smaller and all the points β_n will move toward β_o. The space harmonic phase constant β_1 which is nearest the visible range will eventually obtain a magnitude less than k. When $\beta_1 = -k$ the diffraction occurs in the negative direction (backward wave). If the spacing is further increased the points β_2 then β_3, and so on will enter the circle of radius k, and several oblique waves can result, propagating at angles from the z-direction which may be obtained from the construction shown in Figure 2.

$$\cos \theta_n = \frac{\beta_n}{k} \tag{3}$$

Since the oblique waves carry power away from the grating, the fields near the grating will decrease as a function of distance along the structure. Thus the propagation constants of the fundamental and all of the space harmonics will be complex whenever any of the space harmonics correspond to an oblique wave.

A compact representation of the frequency dependence of the propagation constant is afforded by a plot of frequency versus phase constant. These plots are sometimes called $\omega - \beta$ or $k - \beta$ diagrams or Brillouin diagrams. In this report the ordinate will be the period measured in free-space wavelengths, and the abscissa will be the period measured in wavelengths along the structure.

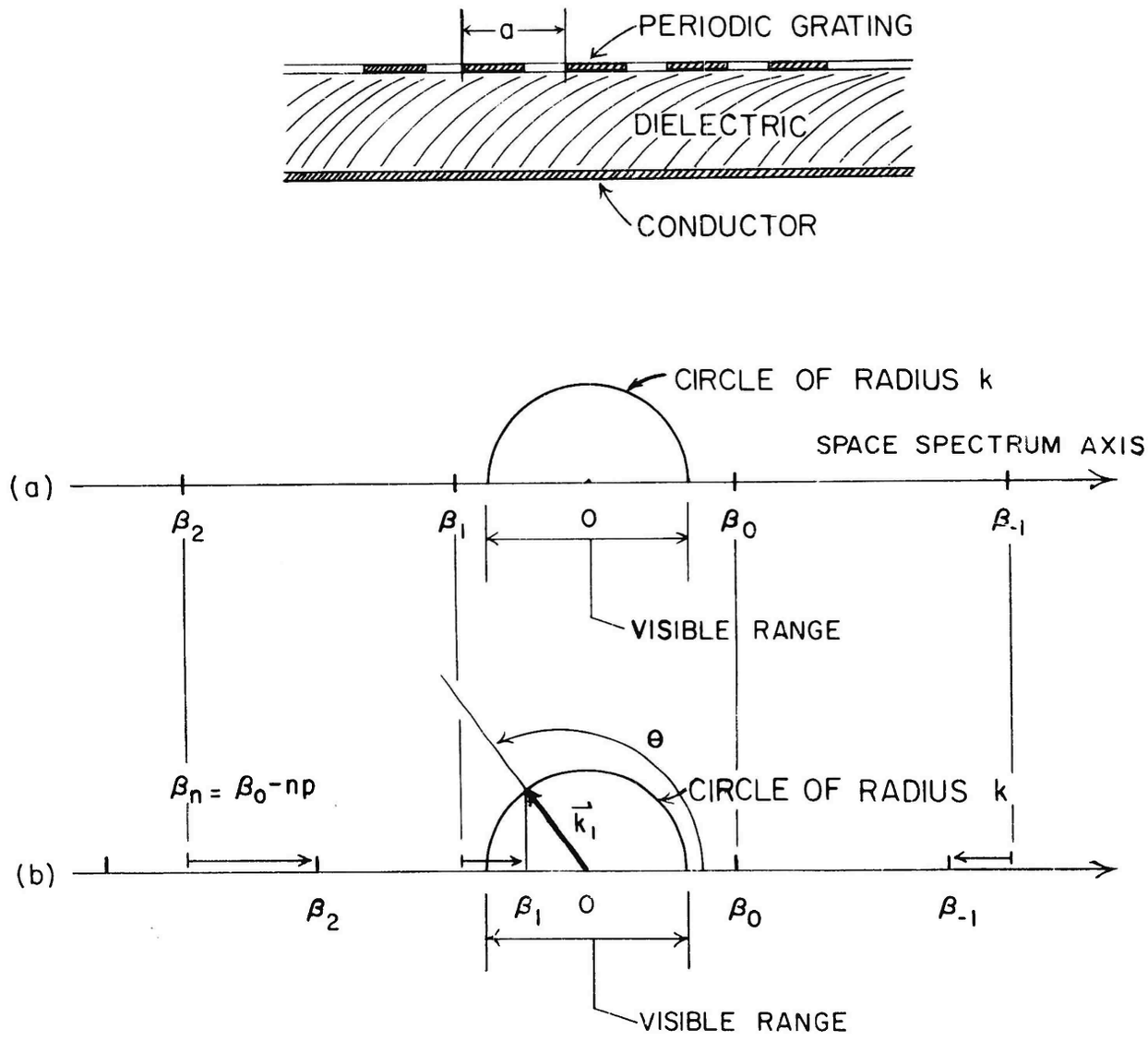

Figure 2. A periodic grating imposed on a slow wave transmission system

If division by p is performed, Equation (1) becomes

$$\frac{a}{\lambda_n} = \frac{a}{\lambda_o} - n \qquad \lambda_n \text{ - wavelength of nth wave} \tag{4}$$

so that the representation of each space harmonic is displaced one unit from that of the fundamental. The condition that all space harmonics be outside the visible range is expressed by

$$\left| \frac{a}{\lambda_n} \right| = \left| \frac{a}{\lambda_o} - n \right| > \frac{a}{\lambda} \quad \text{for all } n$$

and in particular

$$\frac{a}{\lambda} < \frac{a}{\lambda_o} < 1 - \frac{a}{\lambda} \tag{5}$$

This condition is satisfied by all points inside the triangle on the Brillouin diagram shown in Figure 3 A fundamental slow wave is represented by a line whose slope is less than one For small values of a/λ, all space harmonics are far from the visible range, but, as points on the slow wave line approach the right-hand edge of the triangle, the first space harmonic approaches the visible range, and conditions for backward wave radiation are established. The shape of the fundamental phase curve will be modified in the vicinity of the edge of the triangle by coupling between the first space harmonic and a free space wave directed along the structure toward the feed point. Coupling between evanescent space harmonics may also occur within the triangle, distorting the straight line plot shown in Figure 3. The nature of the phase curve in the Brillouin diagram must, of course, be determined for each structure.

Since the propagation constants become complex when a space harmonic enters the visible range, the currents are attenuated. It is therefore possible to build a periodic structure long enough so that the currents are negligible

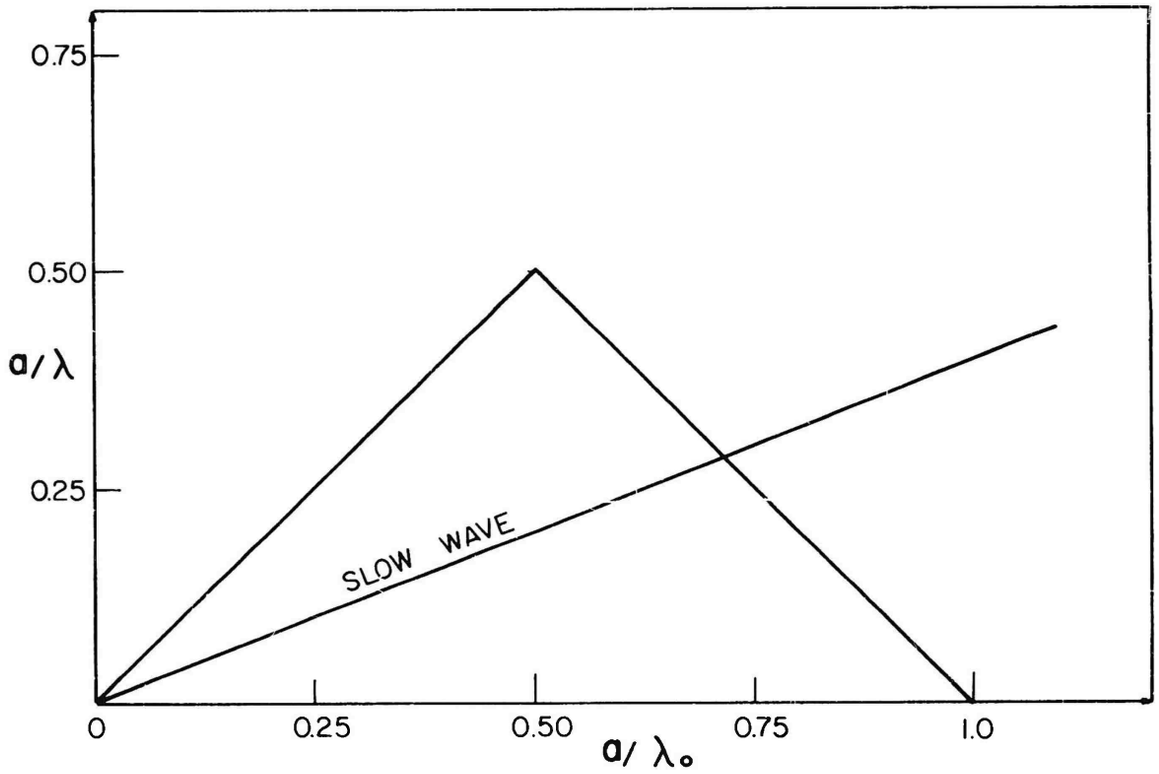

Figure 3. A brillouin diagram showing a slow wave phase constant

at the end. This type of current distribution is very useful for antennas. Again assuming a single fundamental wave the amplitude will be of the form $e^{-\alpha z}$ which gives rise to a radiation pattern given by

$$P(\theta) \quad \frac{1}{1 - jx} \tag{6}$$

where

$$x \quad \frac{k}{a}\left(\frac{\beta}{k} - \cos\theta\right)$$

Unlike the pattern of a uniform amplitude distribution of length L given by

$$P(\theta) \quad \frac{\sin\psi}{\psi}$$

where

$$\psi \quad kL\left(\frac{\beta}{k} - \cos\theta\right)$$

the pattern of Equation (6) has no side lobes. When forward waves are used to produce the radiation field all of the antenna elements are excited by the radiation field. The antenna current distribution in that case experiences a sharp discontinuity at the point where the antenna conductors terminate, as well as at the feed point. When the radiation is due to a backward wave, however, the currents decay with distance from the feed-point and the discontinuity at the opposite end of the antenna will be negligible if the antenna is of sufficient length.

If the antenna is considered as an array of discrete sources instead of the continuous aperture treated above, the pattern is given by

$$P(\theta) \quad \frac{1}{1 - z} \tag{7}$$

where

$$z \quad e^{-\alpha a \cdot jka\left(\frac{\beta}{k} - \cos\theta\right)}$$

The magnitude of Equation (7) is presented in Figure 4 where the exponent is given by

$$-A + j\varphi = -\alpha a + jka\left(\frac{\beta}{k} - \cos\theta\right) \tag{8}$$

The curves of Figure 4 represent universal array factors for arrays having exponentially tapered excitation. The polar plots of radiation patterns for arrays of isotropic sources with this excitation can be obtained from these curves by applying the transformaton between z and θ given in Equation (7). Several patterns deduced from Equation (7) for $\beta/k = 4$ with $A = 0.3$ and $A = 0.6$ are presented in Figure 5. The first pattern ($\frac{a}{\lambda} = 0.187$) is in the excess phase shift range of the Brillouin diagram, i.e., a/λ_o is inside the triangle. At $\frac{a}{\lambda} = 0.2$ the first space harmonic is at the boundary of the visible range. The following patterns depict the frequency scanning that would be expected if the slowness factor, β/k and the attenuation factor α both remain constant with frequency

In a log-periodic grating the period increases progressively with distance along the structure As a wave propagates along the grating it will successively reach points where the various conditions outlined above will occur. If the rate of increase of the period is slow, each small section of the structure will produce about the same complex of diffracted waves as if it were uniformly periodic with the average period of the log-periodic section. For the small periods near one end of the log-periodic grating all space harmonics propagate along the structure. Some distance away, however, the period is correct for a backward wave to enter the visible range. For a slightly larger period this harmonic produces an oblique wave. In this region of the structure the near field will be attenuated as all the space harmonic propagation constants become

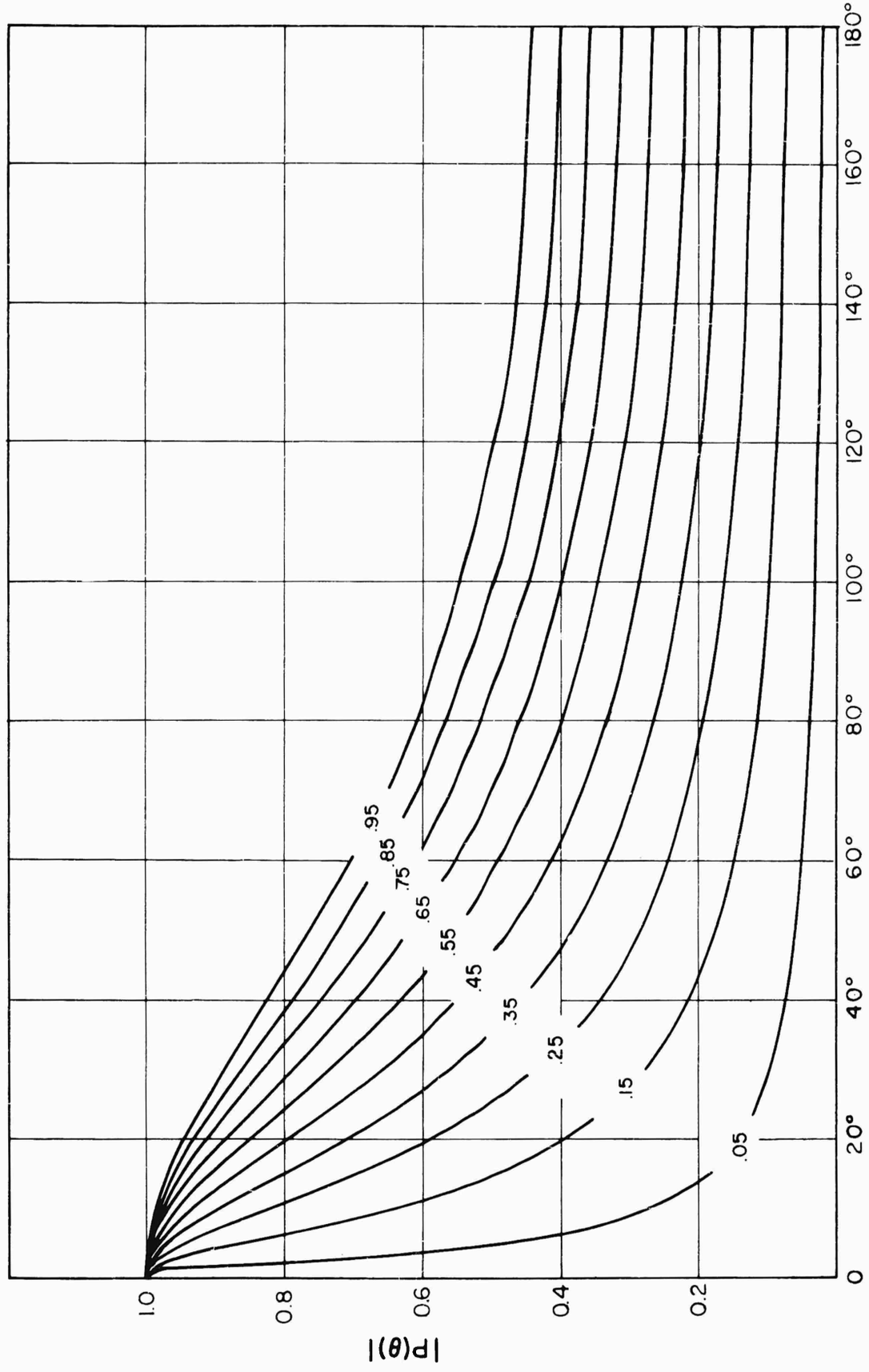

Figure 4. Universal pattern chart for exponential current distributions on discrete arrays

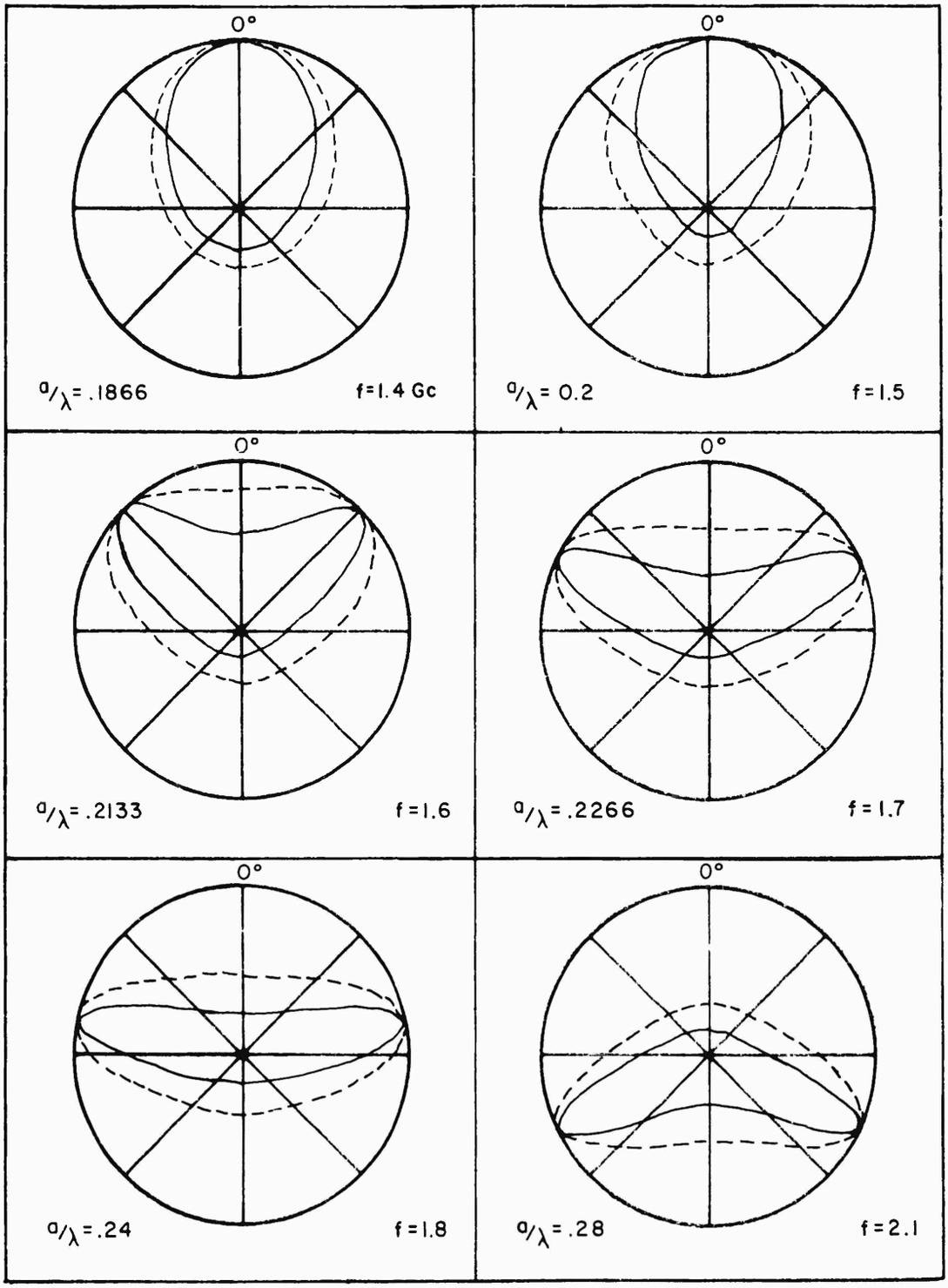

Figure 5. Radiation patterns typical of exponential taper slow wave current distributions $A = 0.3$ ——— $A = 0.6$ — — — —

complex numbers If the coupling is strong enough, the attenuation of the near fields will be almost complete before the periodicity (which results in a backward wave) changes If the coupling is too weak, the currents will penetrate this region and will produce endfire radiation making it impossible to truncate the structure satisfactorily When the frequency is increased the region where the backward wave is produced (which has been called the active region) will move in the direction of decreasing period. When several cells of the periodic structure are included in the active region, the variations with frequency may be quite small, while too large coupling may allow considerable variation within a log-period.

3. HELIX-FED MONOPOLE ARRAY

An array of identical elements (not necessarily the lines of grating) placed periodically along a transmission line and coupled to it will also produce a radiation pattern which can be analyzed as a sum of waves having the $e^{-j\beta_n z}$ dependence on the z coordinate. This may be deduced from Floquet's theorem. While in general several values of β_o, and a sum of the corresponding fields would be required to describe the situation completely, in many practical cases one of these values will correspond to a dominant field and the others can be neglected.

As an example consider the array of monopole antennas connected to a helical delay line as shown in Figure 6. The fundamental wave phase constant can be approximated by considering the current to propagate along the helical wire with free-space velocity. This yields

$$\beta_o = k \csc \Psi \tag{9}$$

where Ψ is the pitch angle of the helix. Since $\csc \Psi > 1$ the fundamental wave is slow.

If the influence of the monopoles on the fundamental wave phase constant is neglected, the element phasing of the array may be approximately determined by periodically sampling the phase of the slow fundamental wave. The sampling rate determines what higher order waves (space harmonics) may be associated with the structure, some of which might be in the visible range. Several waves that agree in phase with a particular sampling of the slow fundamental wave are shown in Figure 7. Because of the multiple-valued nature of phase, the possible values of phase for the fundamental wave are represented by a

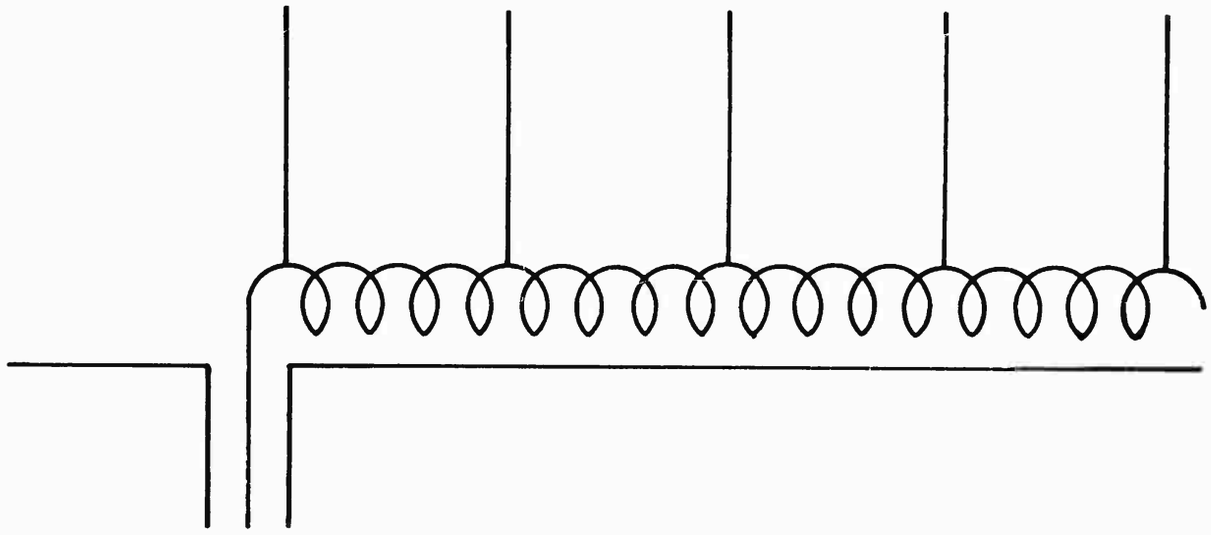

Figure 6. A periodic monopole array with a helical delay line feed

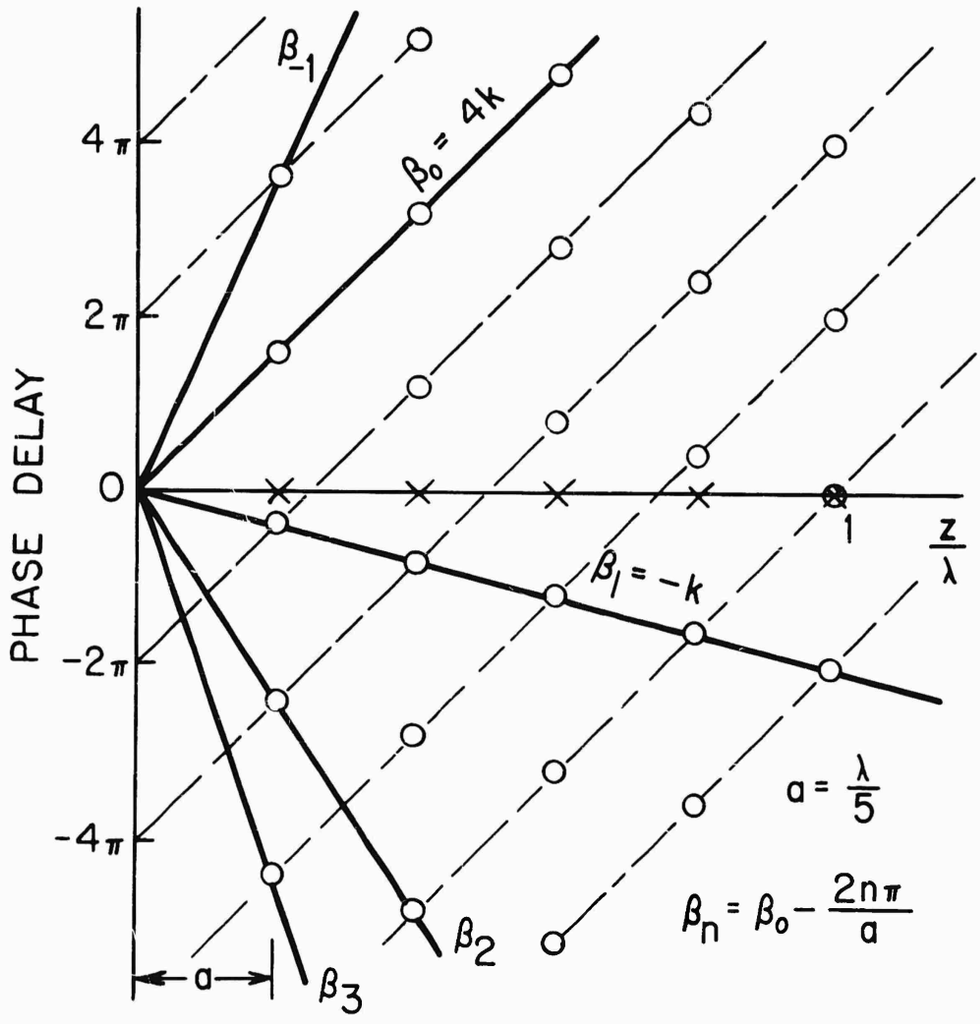

Figure 7. Space harmonics for sampling a slow wave at a specific rate

family of parallel lines displaced by $2n\pi$ radians along the phase axis. Such a family of lines with slope β_o = 4k is shown in Figure 7. We could characterize this fundamental wave by the relative slowness factor, $\beta_o/k = 4$. The phases obtained by sampling with a period a = λ/5 are indicated by small circles on the phase lines for the fundamental wave. Joining the first column of these points to the origin yields the phase lines of the space harmonics. It is noted that the first space harmonic (n = 1) in Figure 7 is a backward wave. All other space harmonics are removed from the visible range. The condition illustrated in Figure 7 is necessary for backfire radiation $\beta_1 = -k$. Other conditions are readily discernable. For broadside, $\beta_1 = 0$ and for endfire, $\beta_1 = k$.

To check the validity of the foregoing simple theory, helix-fed monopole arrays such as that shown in Figure 8 were constructed and tested. The pitch angle of the helix was 18.4 degrees so that the fundamental wave phase constant ignoring the loading effect of the monopoles would be approximately 3.2 k. The helix was wound with number 18 wire on a 9.16-inch diameter fiber tube. On LPM-2 (Uniform Periodic Monopole model 2) 5.7-cm elements were placed every three turns of the helix so that the period of the radiating structure was 4.5 cm. Typical measured azimuthal radiation patterns are shown in Figure 9. Below 1100 Mc the patterns were poorly formed in contrast to the nicely-shaped beams obtained when the backward wave appears. Backward wave radiation is predominant from 1100 to 1500 Mc where the scanning of the beam begins to be discernable. At 1600 Mc two maxima occur at angles with respect to the antenna axis. From the directions of these maxima (52 degrees off axis) the fundamental wave phase constant can be computed as 3.55 k. Evidently then the additional slowing of the fundamental wave is due to the monopoles. The radiation patterns at higher frequencies yield further values of the wavelength of the fundamental wave as given in Table I.

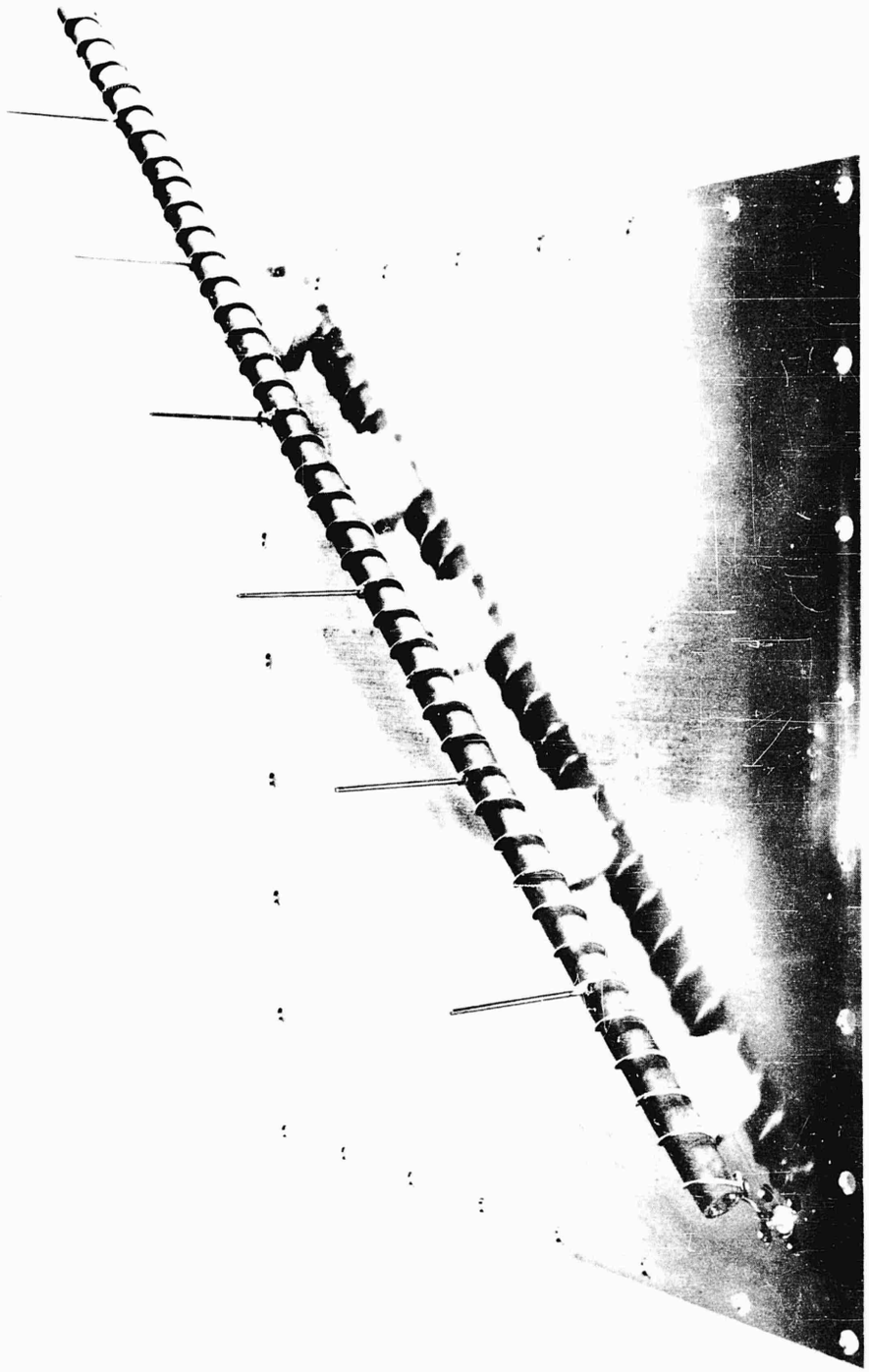

Figure 8. Experimental model of a helix-fed monopole array

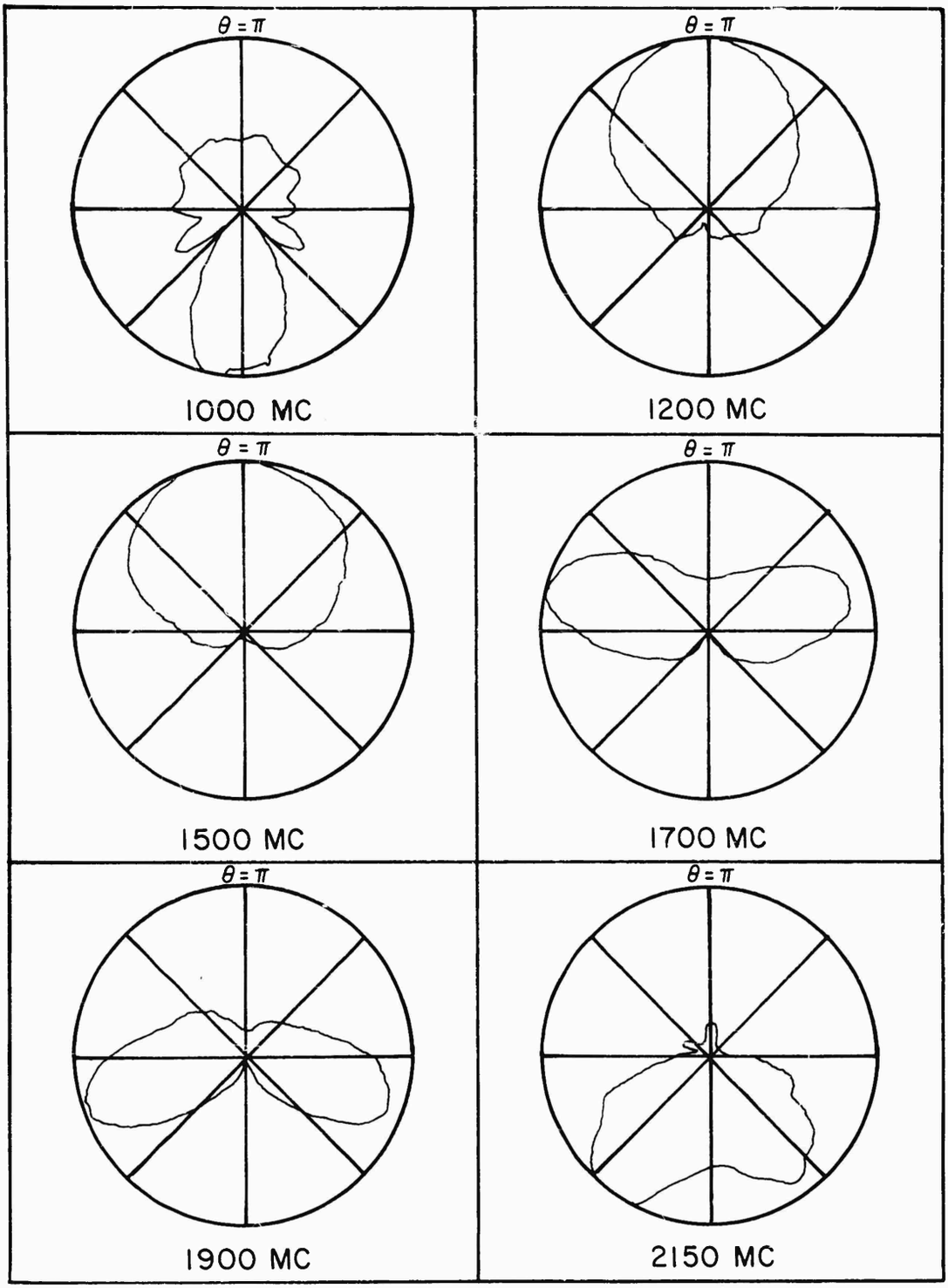

Figure 9. H-plane radiation pattern of a helix-fed periodic monopole array

TABLE I

Beam scanning angle antenna model UPM-2, a = 4.5 cm

Frequency Mc	a/λ	Angle Max.	a/λ_o
1600	0.240	128	0.851
1650	0.247	114	0.900
1700	0.254	105	0.932
1750	0.262	96	0.971
1800	0.270	86	1.02
1850	0.278	80	1.05
1900	0.285	72	1.09
1950	0.292	63	1.13
2000	0.300	55	1.17
2050	0.308	51	1.19
2150	0.322	35	1.26
2700	0.405	152	1.64
2900	0.435	121	1.78

The results listed in Table 2 are for Antenna UPM-2-1/2 which is the model that resulted when alternate elements were removed from UPM-2 All of its parameters are the same as the previous antenna except that the spacing between elements has been doubled.

The above results for the helix fed monopoles lead to the Brillouin diagram of Figure 10. Note that the same ordinate for both antennas occurs at a frequency for UPM-2-1/2 that is half that for UPM-2. This is a direct consequence of doubling the spacing of the monopoles. The broken line on the diagram represents the assumption that the phase velocity measured along a turn of the feed helix is that of free-space; i.e., $\beta_o = k \csc \Psi$. The effect of monopole loading on the propagation constant is shown by the departure of a phase curve from this line. As expected this effect is greater for UPM-2 than for the model with only half as many elements.

It should be noted that between 2150 and 2700 Mc in the case of UPM-2 and between 1200 and 1600 Mc in the case of UMP-2-1/2 there is another frequency band in which no space harmonic is in the visible region. The first space harmonic has scanned from backfire to endfire and departed from the visible region. However, at 2700 Mc (for UPM-2) and 1600 Mc (for UPM-2-1/2) the second space harmonic has entered the visible region. If the fundamental wave velocity is slow enough, the second space harmonic will also scan from backfire to endfire The presence of the second region devoid of oblique waves is indicated in Figure 10 by the second triangle bounded by the lines

$$\frac{a}{\lambda_o} = 1 + \frac{a}{\lambda}$$

and

$$\frac{a}{\lambda_o} = 2 - \frac{a}{\lambda}$$

TABLE II

Beam scanning angle antenna model UPM-2-1/2, a = 9 cm

Frequency Mc	a/λ	Angle Max.	a/λ_o
800	0.240	128	0.850
850	0.255	107	0.926
900	0.270	100	0.952
950	0.285	100	0.953
1000	0.300	92	0.993
1050	0.315	73	1.10
1100	0.330	61	1.16
1150	0.345	53	1.21
1200	0.360	44	1.26
1600	0.478	132	1.68
1700	0.508	110	1.78
1800	0.538	87	2.03
1900	0.568	70	2.19
2000	0.600	53	2.36

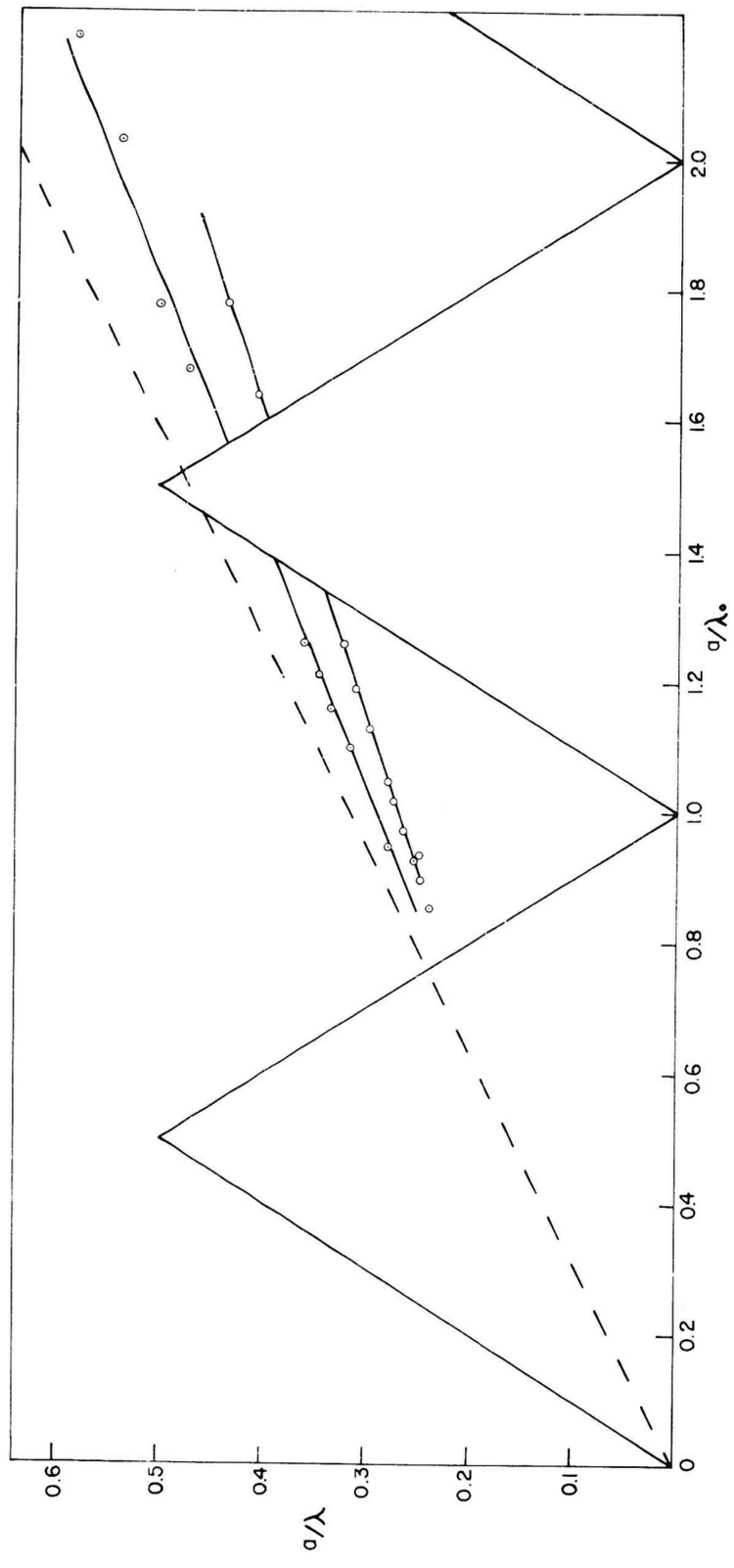

Figure 10. Brillouin diagram for helix-fed monopole arrays

Several tapered or log-periodic models of the helix-fed monopole array were tested with tapers defined by the taper angle α_t in the range from 20 degrees to 6 degrees. The angle α_t is the angle between the axis or center line of the structure and a co-planar line through the outer extremeties of the structure as shown in Figure 11. These structures did not show frequency-independent properties in the range of tapers tested. The performance of models with the smaller tapers, however, was more nearly constant with frequency than that of models with larger taper.

As was indicated in the preceding section, the poor performance of the truncated tapered model for all but the smallest tapers is an indication of weak coupling between the feed wave and the radiated waves. Such loose coupling allows an overly large active region to form. When elements associated with a space harmonic inside the visible region carry appreciable current, energy will be radiated in directions other than backfire. In the case of tight coupling the attenuation constant becomes sizable even inside the triangle of Figure 3, and the elements with appreciable current are all associated with a backward space harmonic. This condition of loose coupling in the case of the uniform periodic structure is indicated by the formation of distinct beams as the frequency is scanned since a large active region is required to form these relatively narrow beams. Where coupling is stronger, the active region on the uniform periodic structure is much smaller giving very broad beams which tend to coalesce into a single beam which widens as frequency is increased. This characteristic is well illustrated by the antennas of the following section.

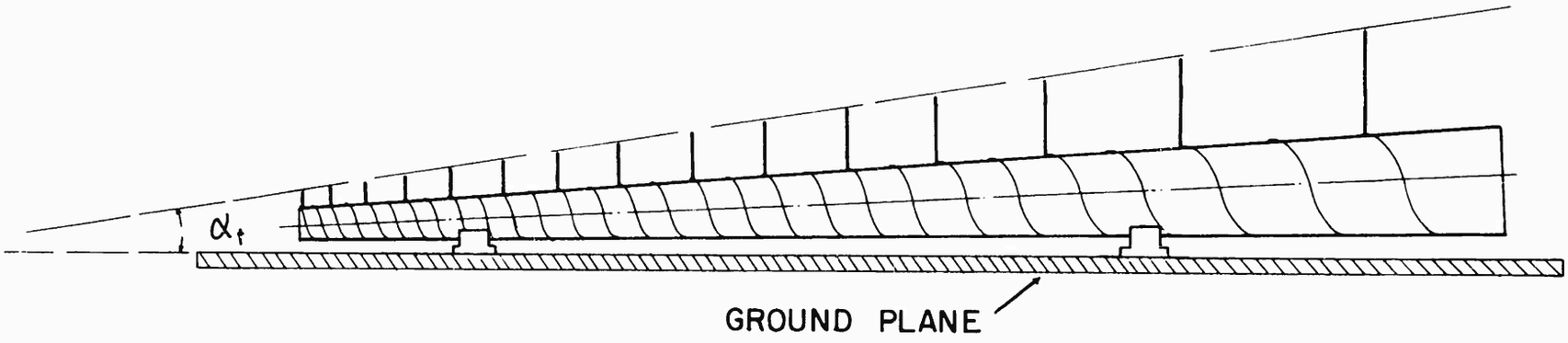

Figure 11. A log-periodic helix-fed monopole array

4 THE ZIG ZAG AND HELIX ANTENNAS

The zig zag and the helical wires shown in Figure 12 are uniformly periodic versions of antennas which have previously been well studied in the log-periodic version. The bifilar helix corresponds to the conical log-spiral antenna[3] The log-periodic zig zag[4,5,6] has been operated as a bifilar antenna in free space and as a horizontally polarized antenna over a conducting ground screen The bent log-periodic zig zag[7] has been shown to be a useful vertically polarized antenna over a conducting ground screen These antennas are constructed of conducting wire following a zig zag or helical path of pitch angle Ψ and period a as indicated in Figure 12.

For the purpose of computing the radiation field produced by oscillating currents in these wires, these periodic structures can be considered to be linear arrays where each cell of the structure is an element of the array Computation of the array factor depends upon the phasing between cells. Once again the assumption of a traveling wave of current on the zig zag or helix proves accurate enough to be useful. If we assume a current wave

$$I(s) = e^{-jks} \tag{10}$$

where k is the free-space phase constant and s is the distance measured along the wire, then the phasing between cells depends upon the length of wire contained in each cell. The phase delay can be characterized by the phase constant

$$\beta_o = k \csc \Psi$$

for the fundamental wave on these structures as was obtained in the preceding section. Division by p yields

$$a/\lambda_o = \frac{a}{\lambda} \csc \Psi \tag{11}$$

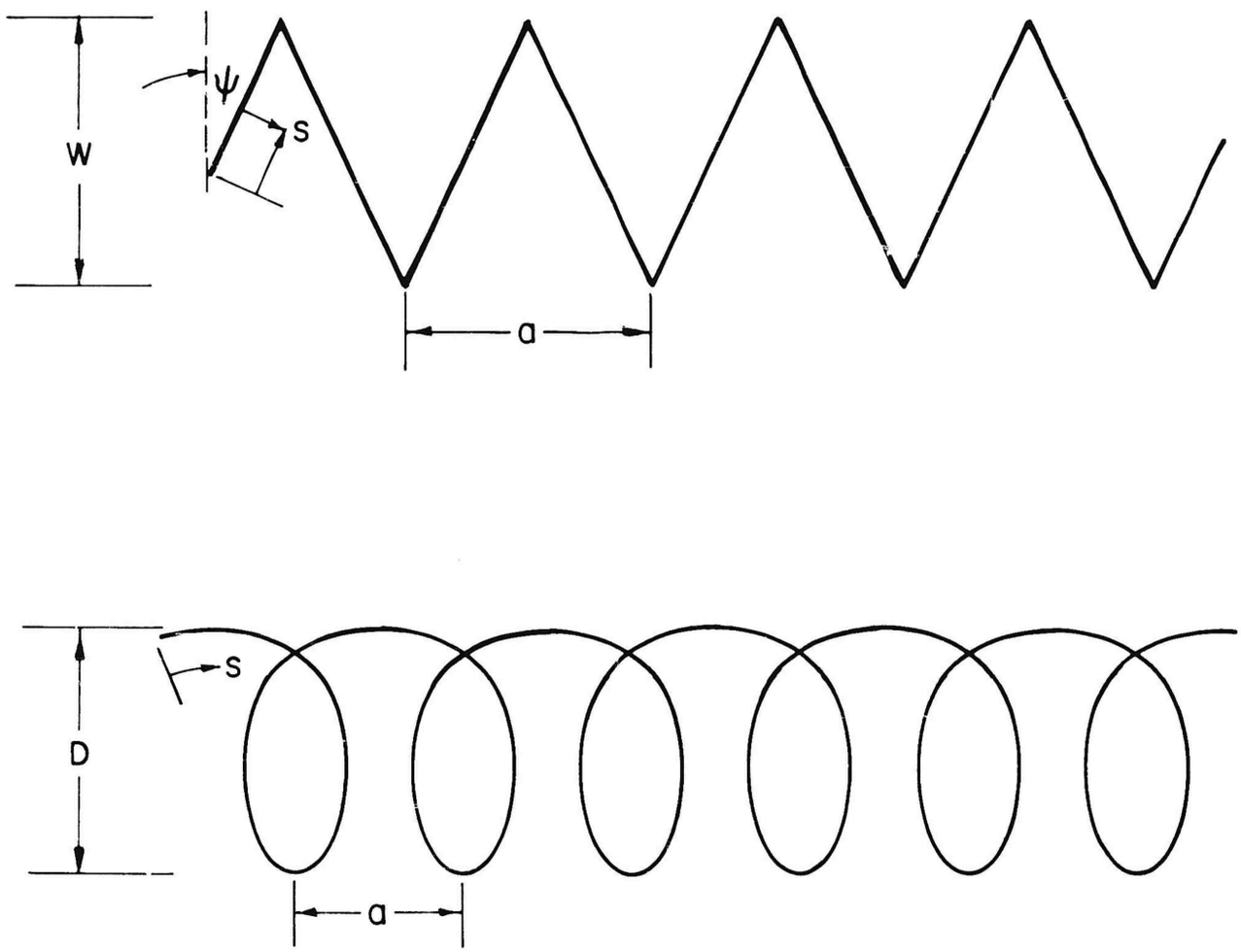

$$\tan \psi = \frac{a}{\pi D}$$

Figure 12. Periodic zig zag and helical wire structures

and by substituting Equation (11) in Equation (5) the condition for backward wave radiation predicted by this approximate theory is seen to be

$$\frac{a}{\lambda} = \frac{1}{1 + \csc \psi} \tag{12}$$

The validity of the foregoing theory, and in particular, the assumption concerning the phase constant of the fundamental wave has been tested by making measurements on monofilar and bifilar zig zag and helical antennas. The monofilar zig zag was fed against a short vertical wire as shown in Figure 13. A Microdot cable was used for the zig zag so that the energy is brought to the feed-point inside the antenna itself. For sufficiently high attenuation of currents along the zig zag, the currents on the outside of the feed cable will become negligible at a short distance from the feedpoint. By measuring the electric vector in the principal E-plane of the antenna, only the field due to the currents on the zig zag will be observed The results of these measurements are shown in Figure 14. From the parameters of the zig zag

$$w = 7.76 \text{ cm}$$

$$a = 4 \text{ cm}$$

$$\psi = 14.5^{\circ}$$

the preceding theory would predict a backward space harmonic entering the visible range at frequency of 1.5 Gc Backward wave radiation would be expected at frequencies somewhat below 1.5 Gc, since the antenna is finite. Strong coupling would also cause the onset of the backward wave at a lower frequency than predicted above The highest gain should occur at these lower frequencies because of the excess phase shift and also because the small attenuation of current at these frequencies allows a deeper penetration of currents into the structure

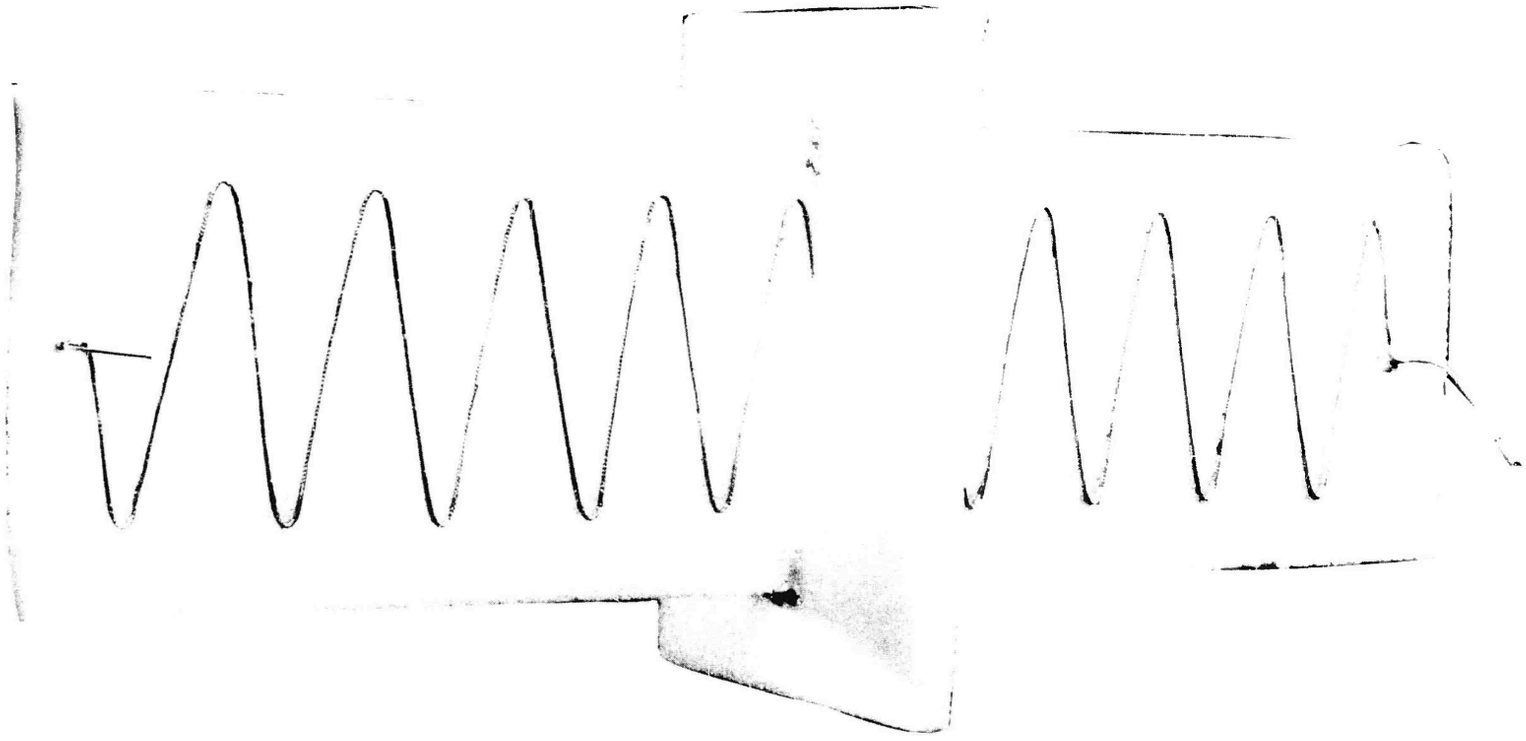

Figure 13. A monofilar zig zag wire antenna

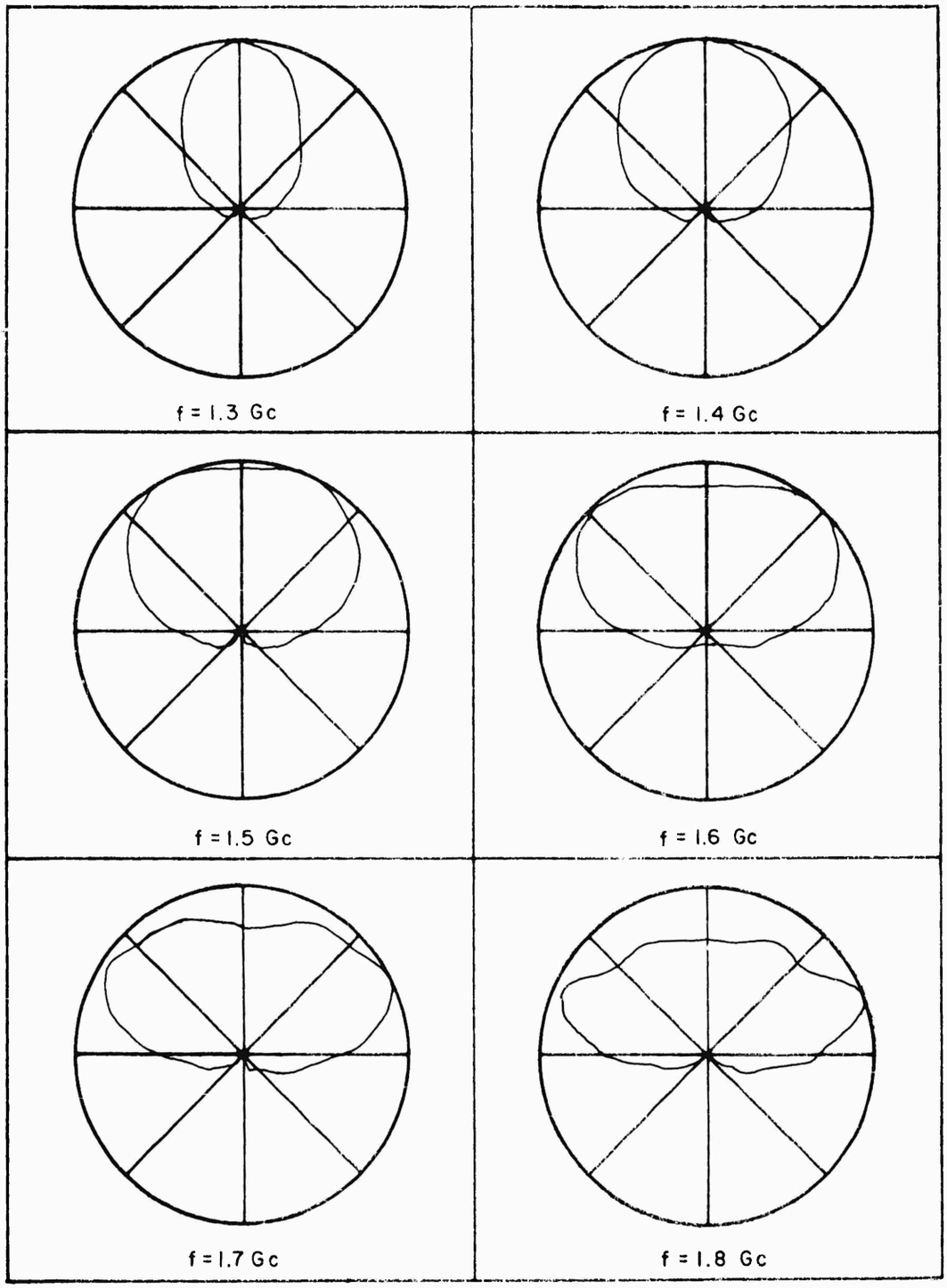

Figure 14. H-plane radiation patterns of a monofilar zig zag antenna

A number of bifilar zig zag antennas have also been tested. In this case the detector (bolometer or crystal) was mounted directly at the feedpoint of the antenna, and the antenna conductors were used to conduct the audio signal (1000 cycle square wave modulation) to the recorder With this method of feed it was a simple matter to truncate the antenna at a number of successively decreasing lengths and obtain an estimate of the depth of penetration of currents on the antenna The results of this series of measurements are shown in Figure 15. It is readily observed that the current is practically negligible beyond the fourth cell since the pattern obtained with 3 or more cells remains unchanged

According to the approximate theory a bifilar zig zag antenna with the same parameters as given above would also have a backward space harmonic at 1500 Gc as before Below this frequency the pattern should be highly directive, and above this frequency the maximum of the beam should scan away from backfire, through broadside, to endfire The actual performance of this antenna is shown in Figure 16

Several factors which are quantitatively unknown at present may serve to explain deviations from the simple theory. At the lowest frequency there is a small lobe in the endfire direction. This is probably evidence of end effect on the antenna If the current wave on the structure is not sufficiently attenuated, it will be reflected from the open end of the structure. This reflected current wave will produce backward wave radiation, but in the endfire direction The length necessary to avoid this end effect at any given frequency is dependent upon the attenuation of the currents The dependence of the attenuation upon the parameters of several different structures is a subject of continuing investigation at our laboratory This attenuation also governs the shape of the patterns at the higher frequencies

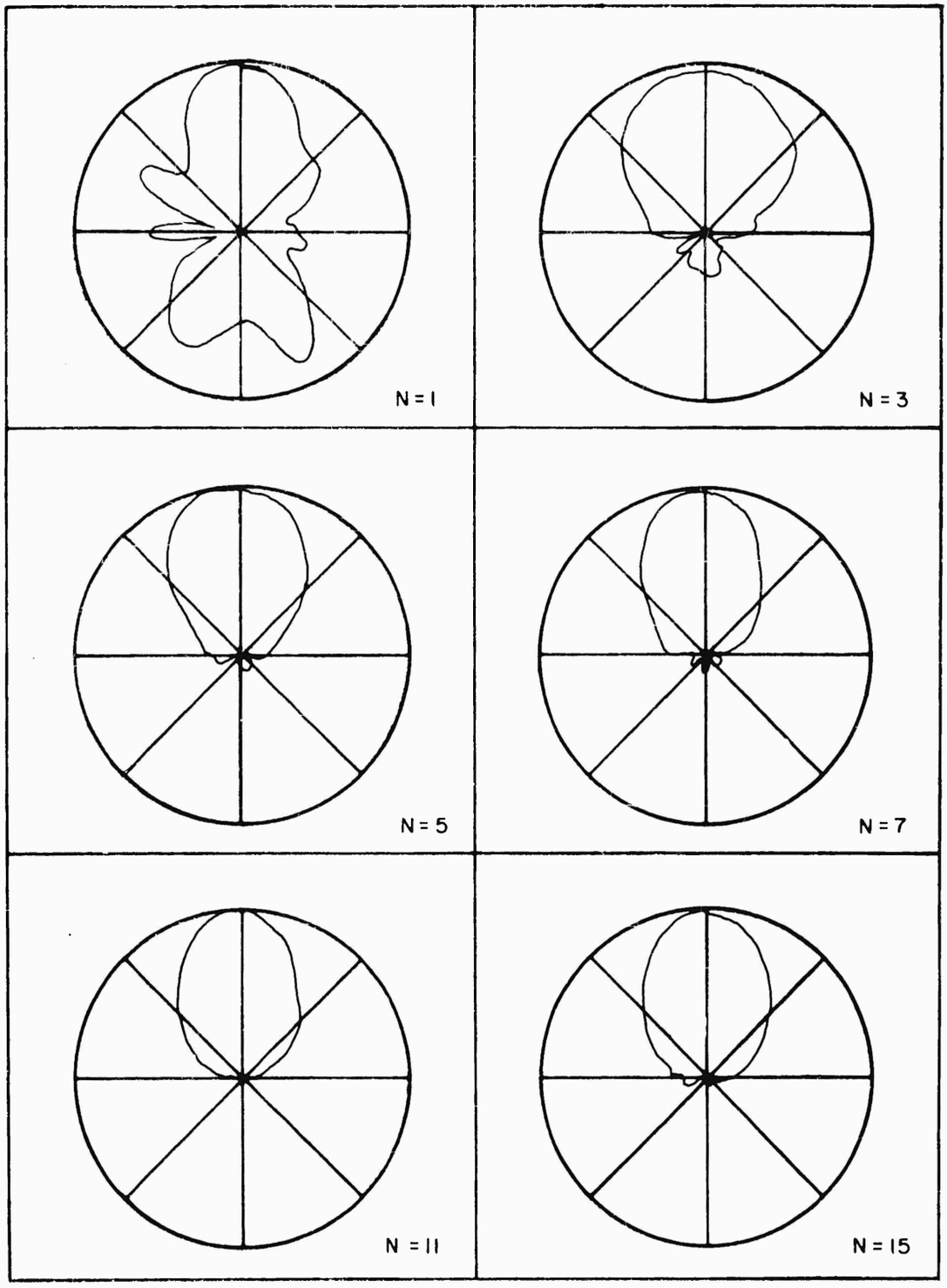

Figure 15. H-plane radiation patterns of a bifilar zig zag antenna as a function of number of cells

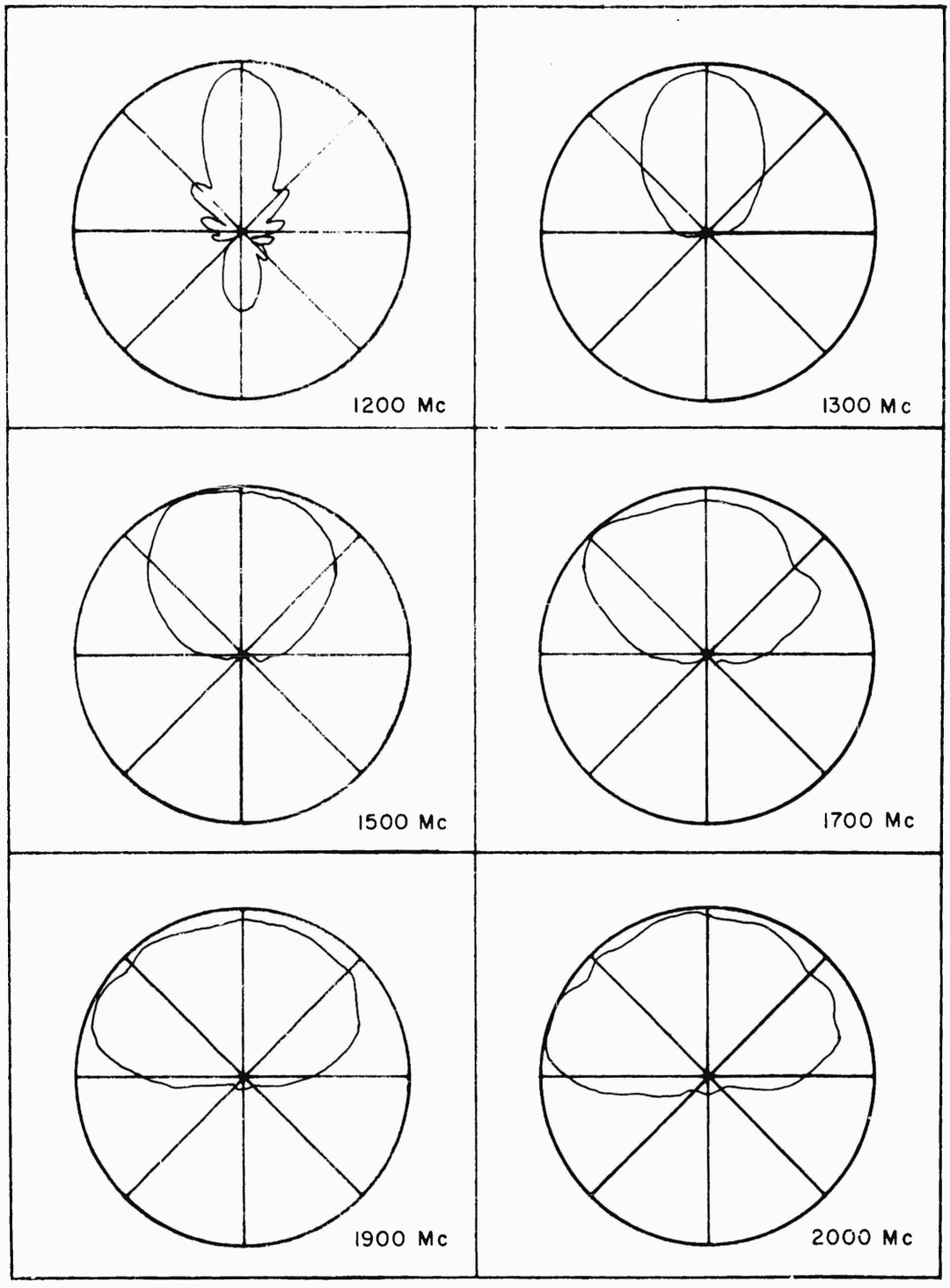

Figure 16a. H-plane radiation patterns of a bifilar zig zag antenna as a function of frequency
Pitch = 4 cm, Pitch width = 7.76 cm, Pitch angle = 15^{o}

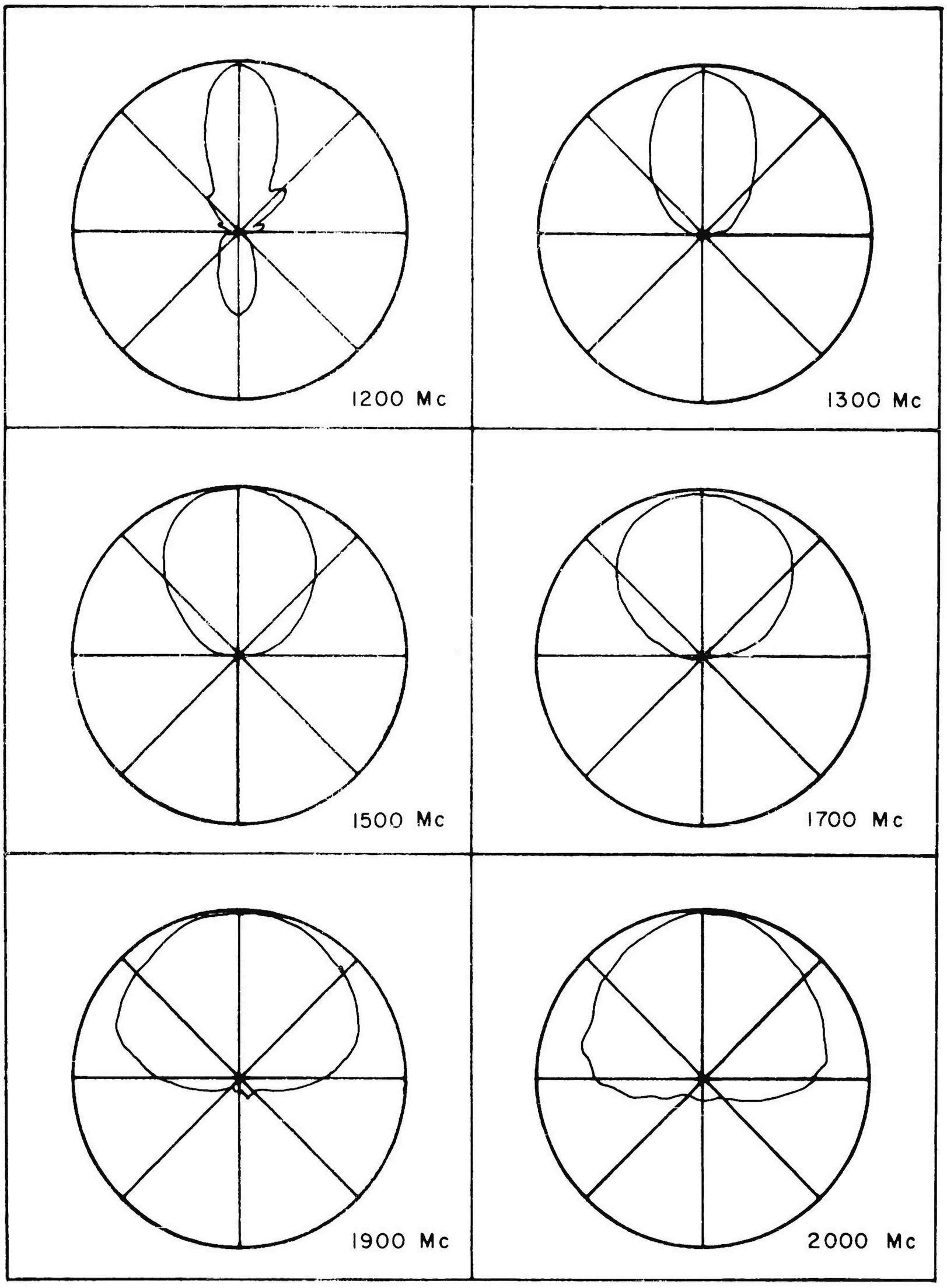

Figure 16b. E-plane radiation patterns of a bifilar zig zag antenna as a function of frequency
Pitch = 4 cm, Pitch width = 7.76 cm, Pitch angle = 15^{o}

As mentioned before the approach of space harmonics near to the visible range will modify the fundamental wave phase constant. This modification will involve a variation in the phase constant previous estimated by Equation (9) as well as the appearance of an attenuation constant. Furthermore, there may be other fundamental wave constants for the zig zag wire in addition to the one given by Equation (9) which we have assumed here to be predominant.

The measurements described above have also been made on monofilar and bifilar helix antennas and similar results have been obtained. The zig zag and helical antennas operating in the backfire condition have a smaller cross section in terms of the wavelength than the conventional endfire zig zag and helical antennas.

A Brillouin diagram for the bifilar zig zag is shown in Figure 17. The broken line results from the assumption of propagation at free-space velocity along the wire This curve is given by

$$\frac{a}{\lambda_o} = \frac{a}{\lambda} \csc \psi$$

The measured points on Figure 17 were determined by establishing a standing wave on the zig zag and measuring the distance along the axis between nulls. The standing waves were produced by a short circuiting plate 60 inches square at the end of a zig zag with 15 cells. At $\frac{a}{\lambda} = 0.2$ the current distribution begins a transition from a standing wave to a rapidly decaying wave. Some typical records of the near field measurements are shown in Figure 18. A value of $\frac{a}{\lambda} = 0.2$ corresponds to the frequency at which backfire radiation patterns are observed from this zig zag antenna

The Brillouin diagram in Figure 17 is different from others appearing in this report in that the phase curve does not start at the origin of the diagram.

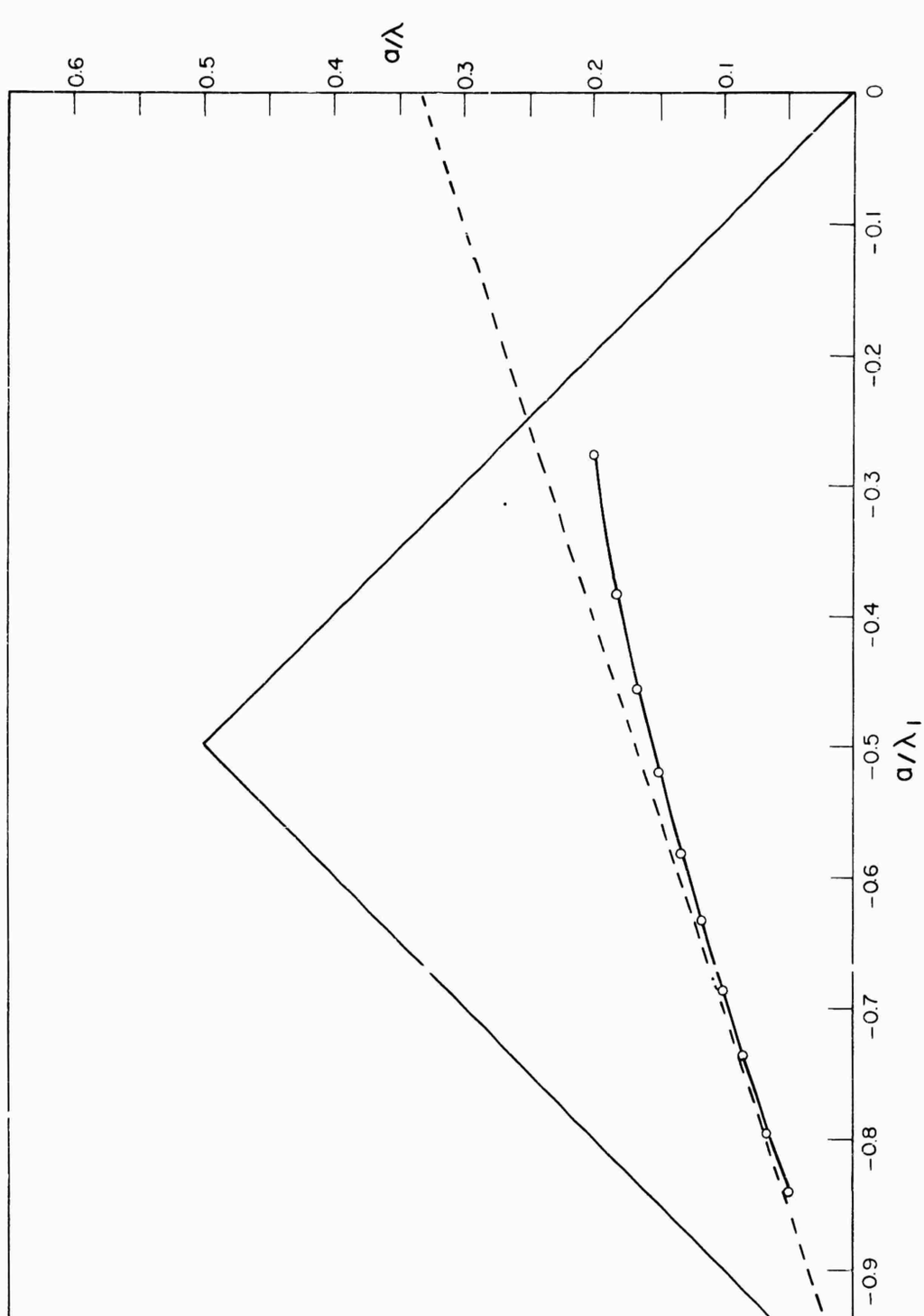

Figure 17. Brillouin diagram for a bifilar zig zag

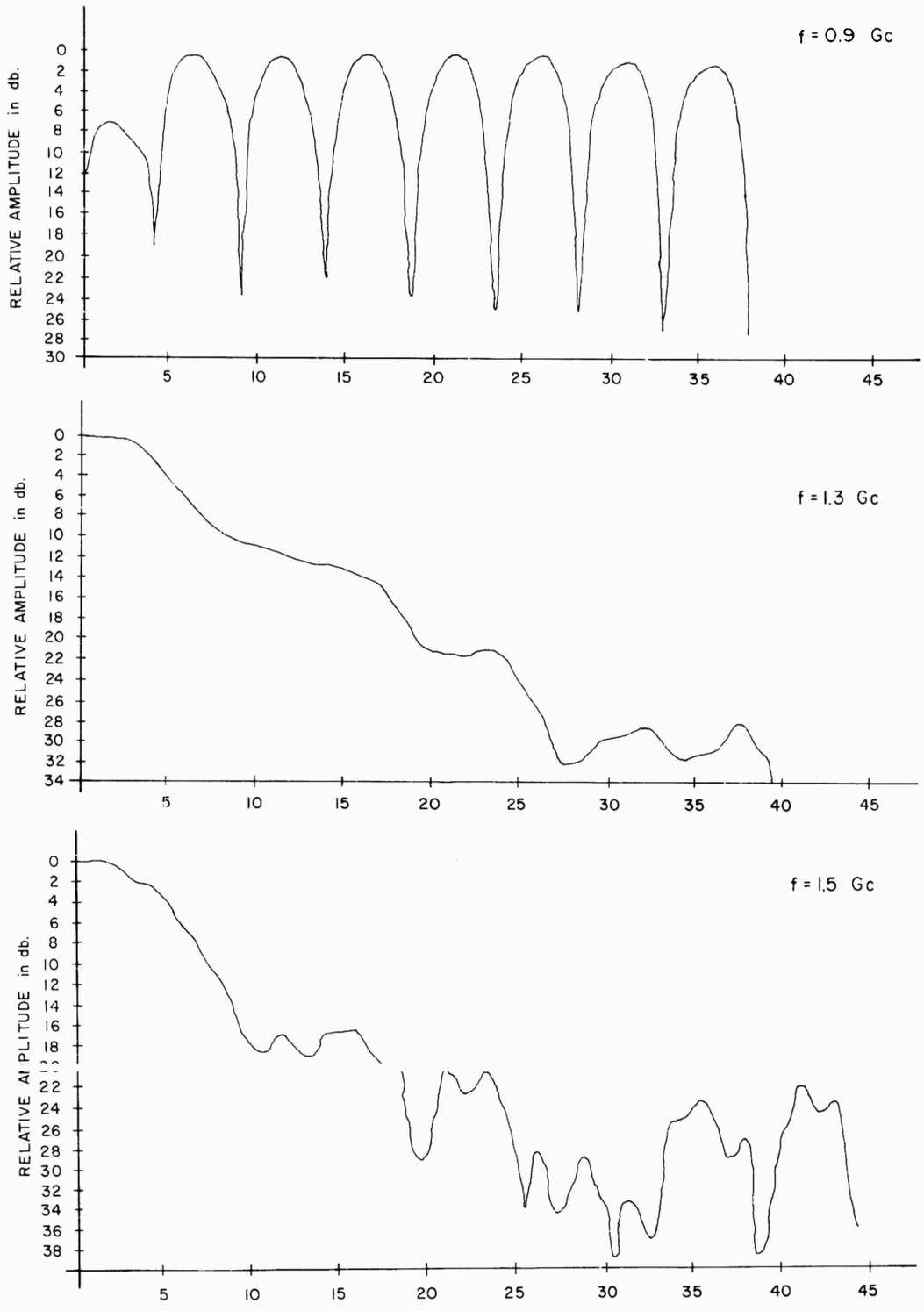

Figure 18. Current amplitude distribution for a bifilar zig zag antenna
Pitch = 5 cm, Pitch width = 7.07 cm, Pitch angle = 19.5°

This is a characteristic of the backward wave. The Brillouin diagram represents one cell of a periodic figure; each cell is called a Brillouin zone. It has been the practice here to use that zone which most nearly corresponds to the been the practice here to use that zone which most nearly corresponds to the measured results. In the case of Figure 17 the curve is plotted in the n = -1 zone to indicate the observed phase progression toward the feed point. This curve also indicates that the wave length along the structure increases with frequency from a minimum at zero frequency given by the period of the structure. This corresponds to the plus minus polarity change along the structure that would be observed if the structure were excited by direct current.

Several log-periodic versions of the zig zag antenna have been studied[4]. The bifilar log-periodic zig zag antenna is shown in Figure 19. Figure 20 is a typical radiation pattern of this antenna. The monofilar horizontally-polarized zig zag antenna is shown in Figure 21 with typical patterns in Figure 22. Several models of the vertically-polarized bent zig zag[4] are shown in Figure 23. The evidence of Figure 15 shows that the currents on a zig zag wire are highly attenuated when the coupling between the backward space harmonic and the free space wave occurs. Hence, it is to be expected that it should be possible to convert this periodic structure into a frequency independent antenna by applying a taper. Furthermore, the angle of taper need not be kept very small in order that the log-periodic variations in performance be smoothed out.

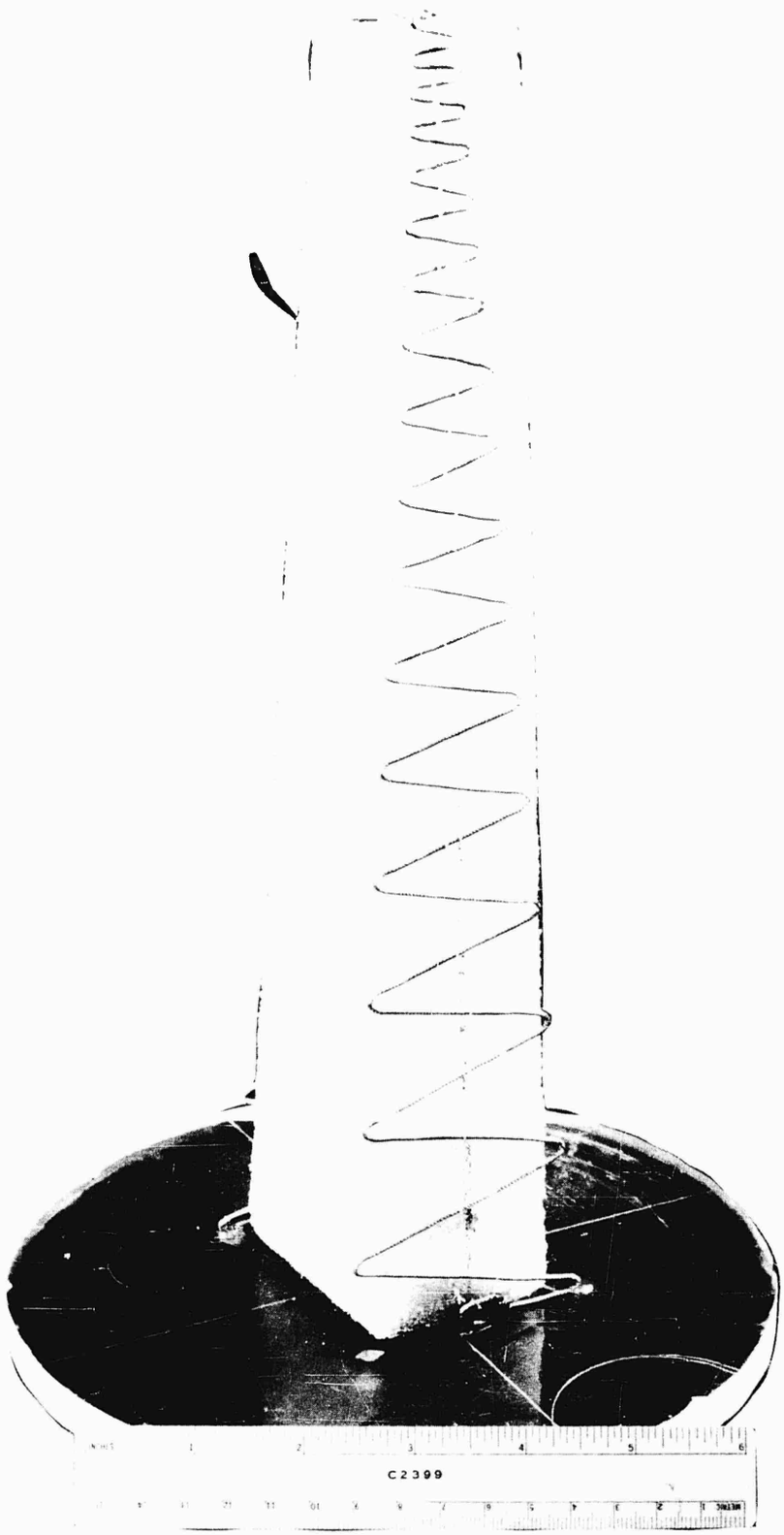

Figure 19. A log-periodic bifilar zig zag antenna

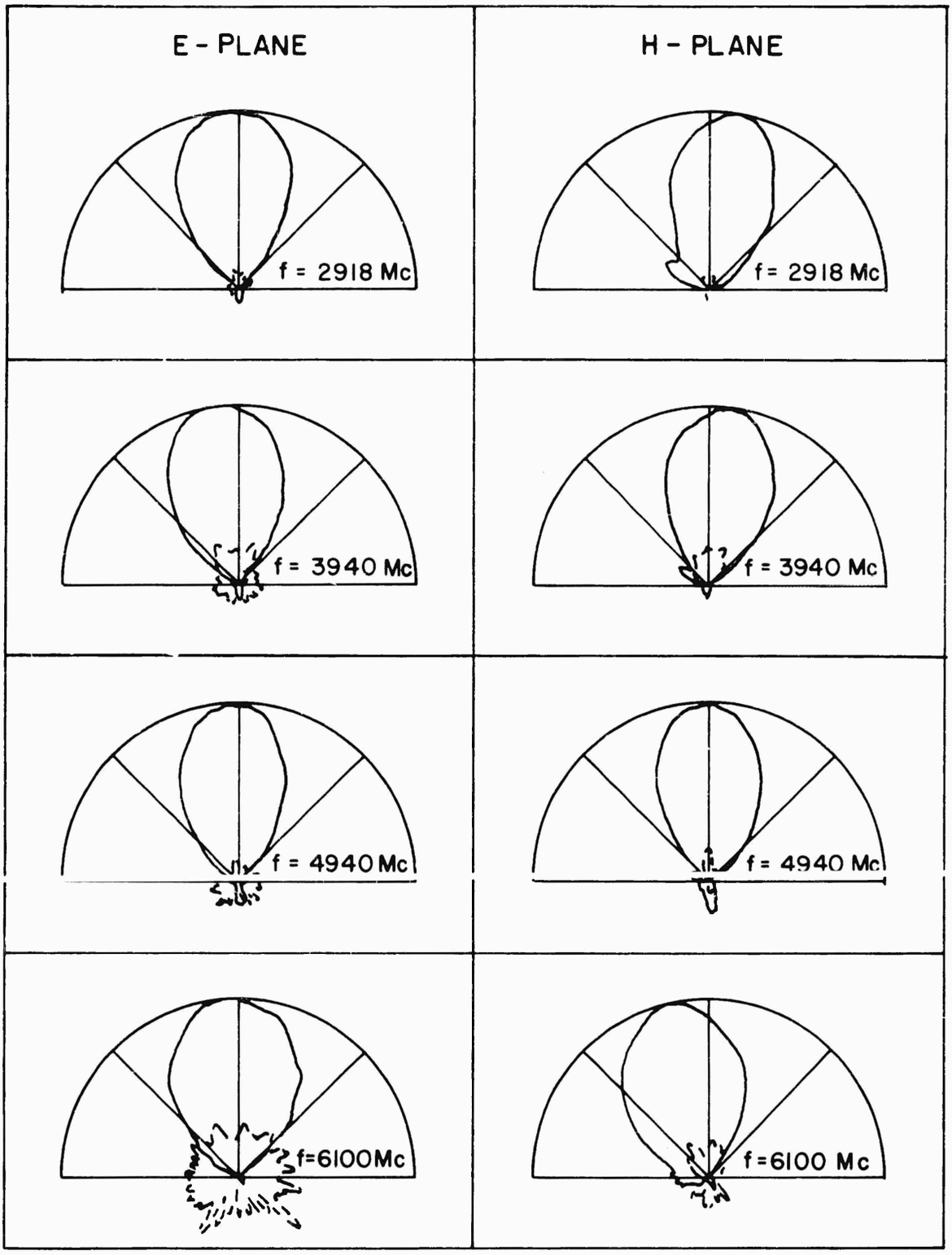

Figure 20. Radiation patterns of a log-periodic bifilar zig zag antenna

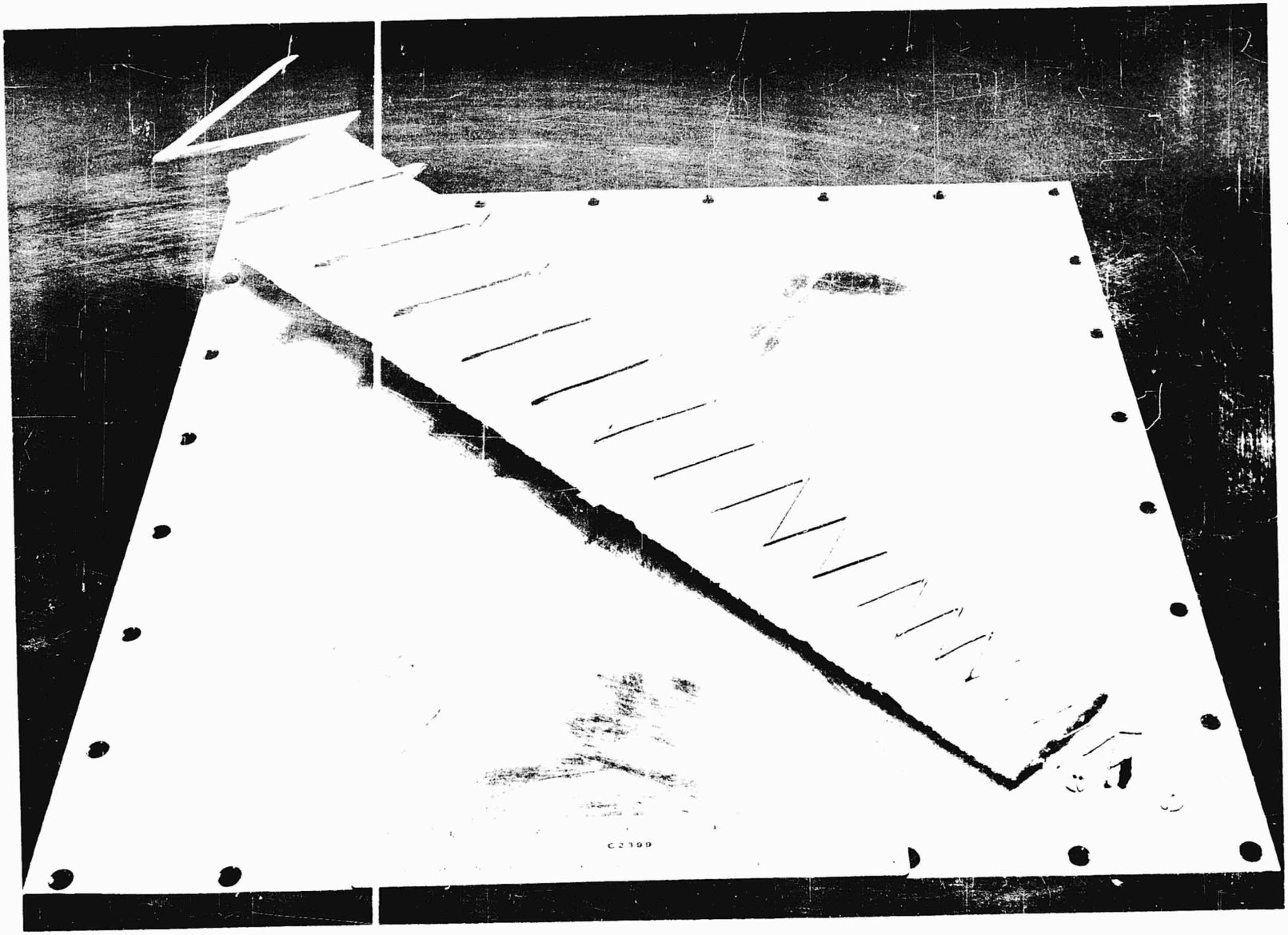

Figure 2 . A log-periodic monofilar zig zag over ground

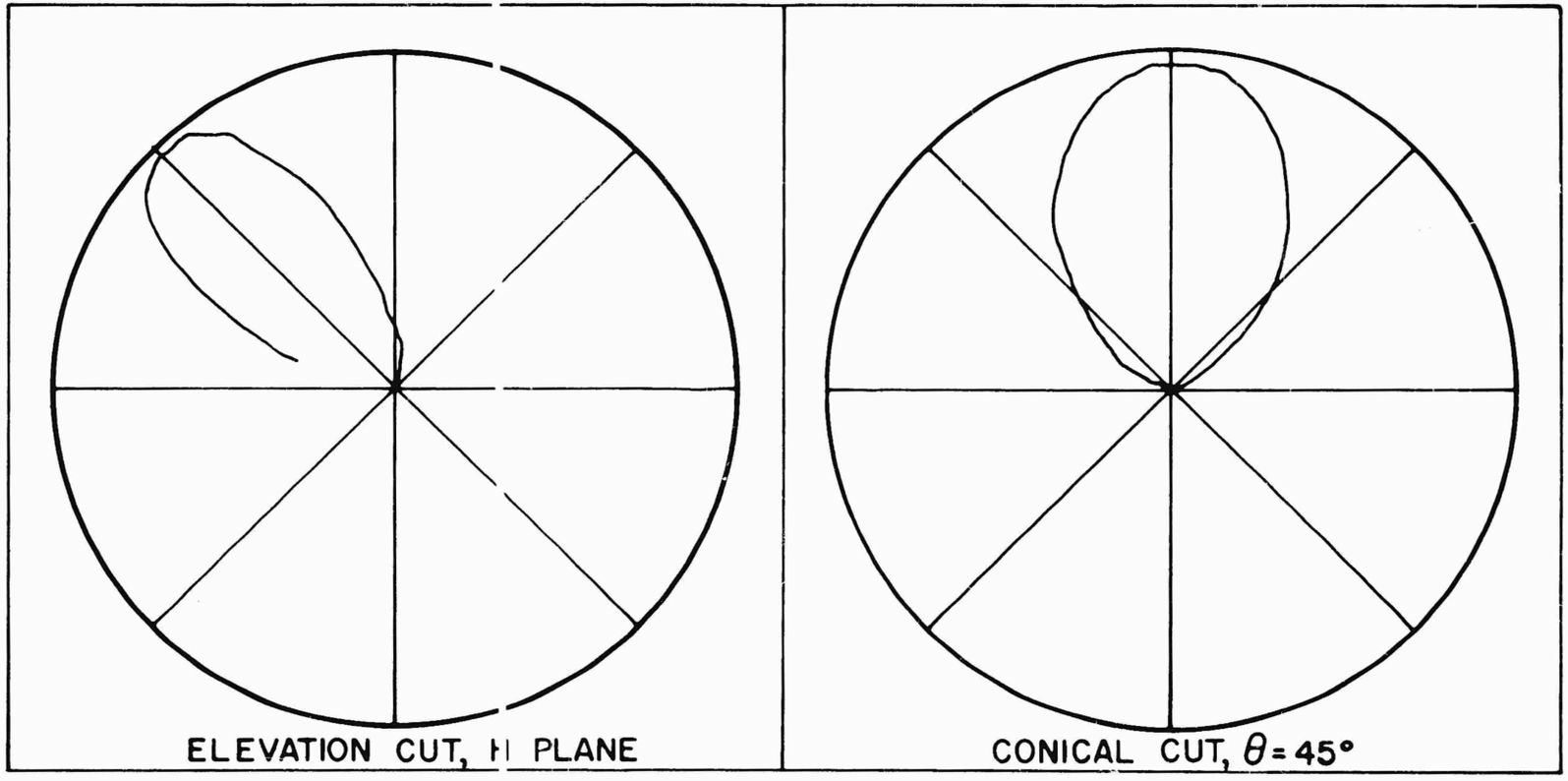

Figure 22. Radiation patterns of a log-periodic monofilar zig zag over ground

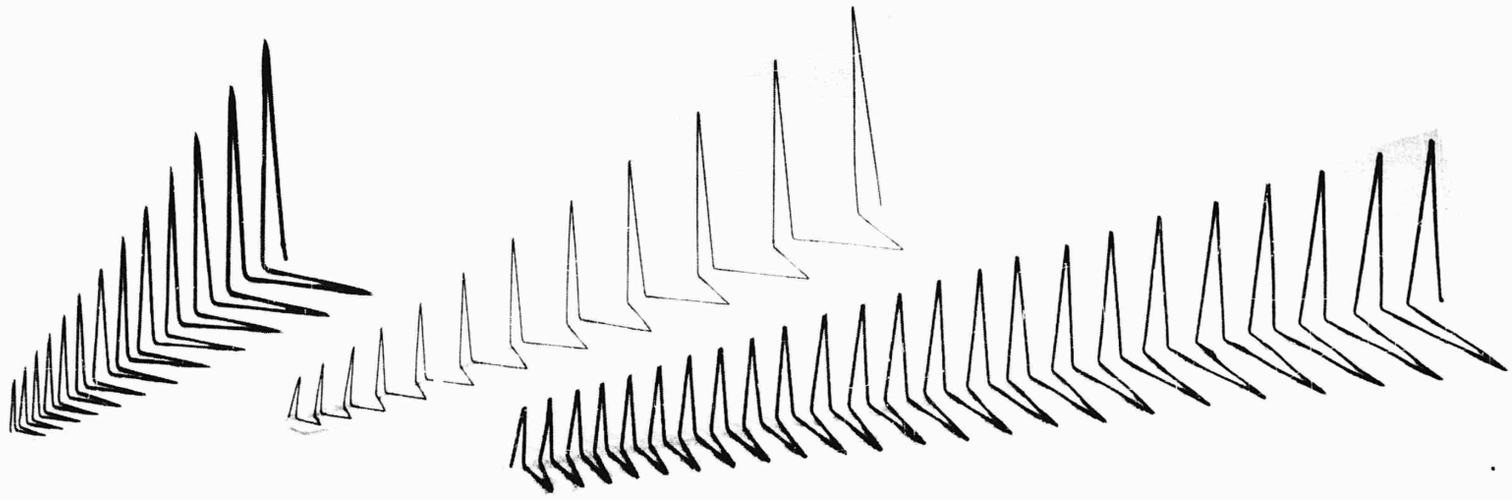

Figure 23. Vertically-polarized log-periodic zig zag over ground

5. PERIODIC STRUCTURES WITH RESONANT ELEMENTS

The periodic zig zag and helix antennas have similar Brillouin diagrams. They are both characterized by a perturbation of the slow wave line shown in Figure 3. The perturbation occurs at the boundary of the triangle where the first backward space harmonic crosses into the visible region. It is interesting to note that one structure serves dual functions as transmission line and radiating elements in both the zig zag and the helix. There are other periodic structures which make excellent frequency independent antennas in the tapered (log-periodic) version and yet which have a different type of Brillouin diagram. The periodic dipole array shown schematically in Figure 24 is the foremost example of this type[7]. In this case the functions of transmission line and radiating element are performed by distinct, although interacting, elements.

The Brillouin diagram of the periodic dipole array is characterized by certain frequency bands where waves can propagate along the structure with essentially undiminished amplitude. In other bands rapid attenuation of the feeder current occurs even though the phase constant of the currents along the feeder corresponds to a point in the interior of the triangle, far removed from the boundary. The periodic loading of the transmission line in this case evidently produces an effect analogous to periodic loading in a waveguide. In the latter case passbands and stopbands alternate in the frequency spectrum. In the stopbands the propagation constants of all the space harmonics are complex and energy does not penetrate a large distance into the structure.

Typical feeder voltage plots obtained on a uniform periodic dipole, using the short-circuit termination as previously described, are shown in Figure 25

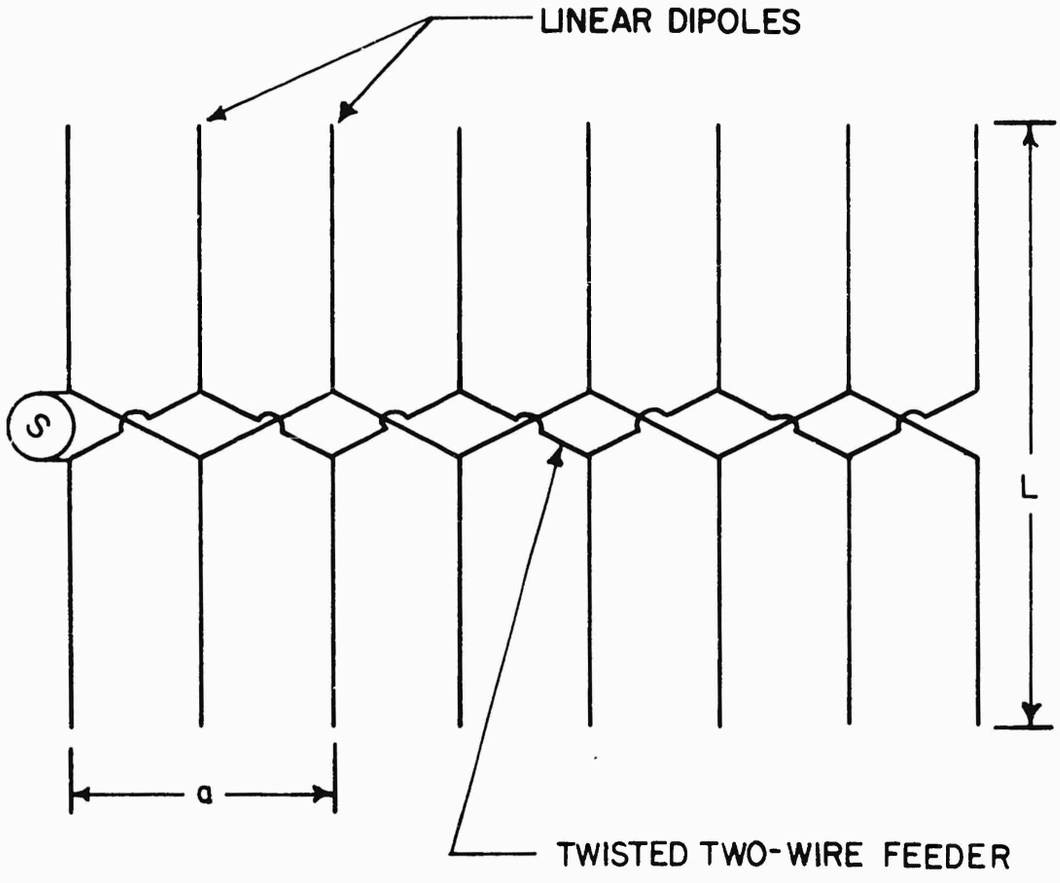

Figure 24. A periodic array of dipoles

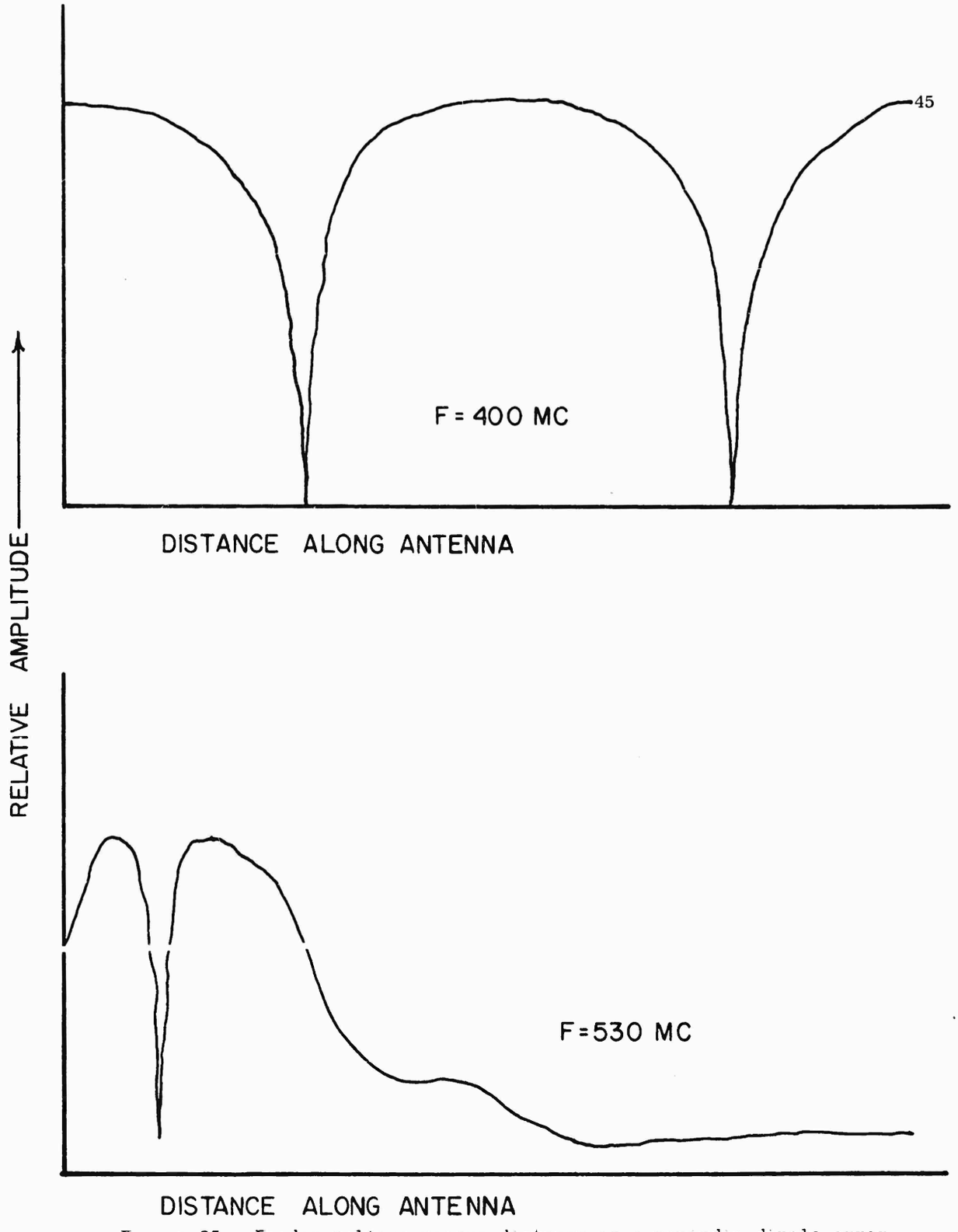

Figure 25. Feeder voltage versus distance on a periodic dipole array

From the standing wave characterized by the deep nulls at 400 Mc it is apparent that this frequency is in the passband of the structure. At 530 Mc, however, the field decays so rapidly that the short-circuit no longer influences the near-field distribution. This indicates that 530 Mc is in the stopband. The Brillouin diagram constructed from a series of such plots is shown in Figure 26. The slant line in Figure 26 represents a wave with free-space velocity. At low frequencies a slow wave propagates along the dipole array. As we approach the half-wave resonant frequency, however, the slowness increases quite rapidly with increasing frequency so that the group velocity $\frac{d\omega}{d\beta}$ is very small. In infinite closed periodic structures the phase constant curve continues to the center of the triangle ($a/\lambda_o = 0.5$) at which point the group velocity is zero (point A in Figure 26). The propagation constant for all space harmonics becomes complex at this point and the phase constant remains fixed while the attenuation constant varies with frequency inside the stopband. The phase shift per cell of each space harmonic inside the stopband is some multiple of π radians. The stopband is produced by coupling between forward and backward waves on the structure rather than by coupling to a free-space wave. In the dipole array this coupling is predominant near the resonant frequencies of the elements. The Brillouin diagram for the finite length dipole array can be expected to be perturbed somewhat from the idealized case of the infinite, lossless periodic structure.

Above the first stopband is another passband similar to the one at lower frequencies except that the wave on the line is fast over a portion of the band. Even though the phase velocity along the line is fast, there is little radiation in this band because of the twisted feeder shown in Figure 24. The phase velocity corresponding to the dipole excitation remains slow. At the frequency

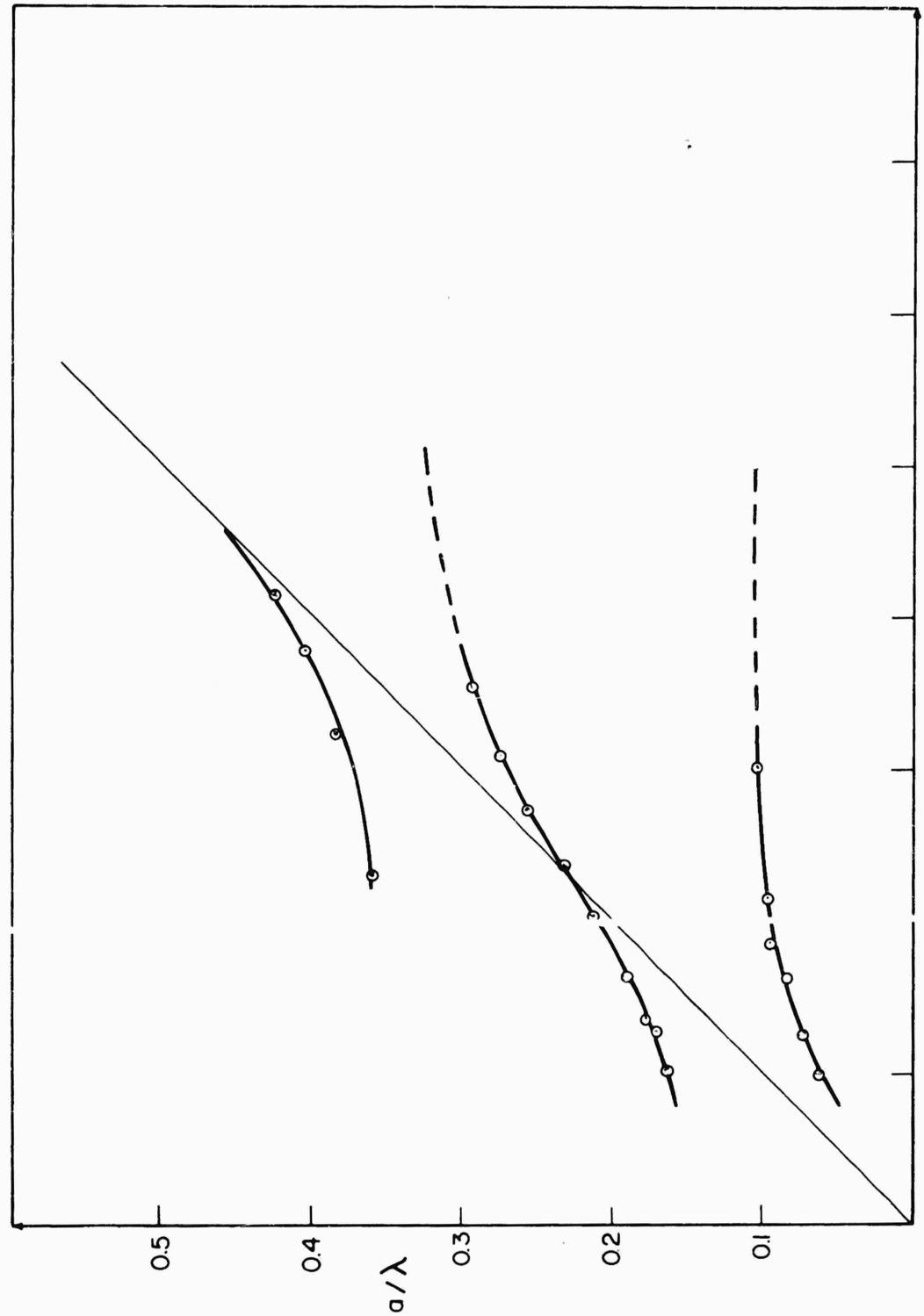

Figure 26. Brillouin diagram for feeder voltage on a periodic dipole array

where the dipoles again possess resistive input impedance (near one wavelength) the velocity along the line reduces to the free-space value. Above this frequency the feeder wave is again slow; the velocity diminishing rapidly as the edge of another stopband is approached. The properties of the second stopband are similar to the first except for being located near the frequency where the elements are three half wavelengths long. The number of stopbands displayed by a particular dipole array depends upon the density of dipoles. Increasing the number of dipoles increases the capacitive loading per unit length at the lower frequencies and thereby influences the phase velocity. This in turn makes it possible for several resonances of the dipoles to occur within the frequency span limited by $0 < \frac{a}{\lambda} < 0.5$. Applications of this phenomenon have been made to multi-band antennas[10].

The radiation patterns of the uniform dipole array are essentially the same as those obtained from other periodic structures having exponential current distributions. In passbands the pattern is multi-lobed as expected from a standing wave excitation of the dipoles. In the stopbands, however, a well-formed unidirectional beam is obtained. Patterns of the uniform dipole array which are typical of the passband and stopband are shown in Figure 27.

The essential role of the twisted feeder in producing the backfire radiation pattern is illustrated by means of the series of Brillouin diagrams described below. Consider first the idealized diagram shown in Figure 28a. Let us suppose that this gives the phase constant of the feeder current, $\beta_o = \frac{2\pi}{\lambda_o}$. Even though these results were measured for the feeder voltage rather than current, the phase progression of both on an infinite structure should agree. The phase shift from cell to cell would be $\beta_o a$. The phase shift in the current from one dipole to the next would be half this value However, at each dipole

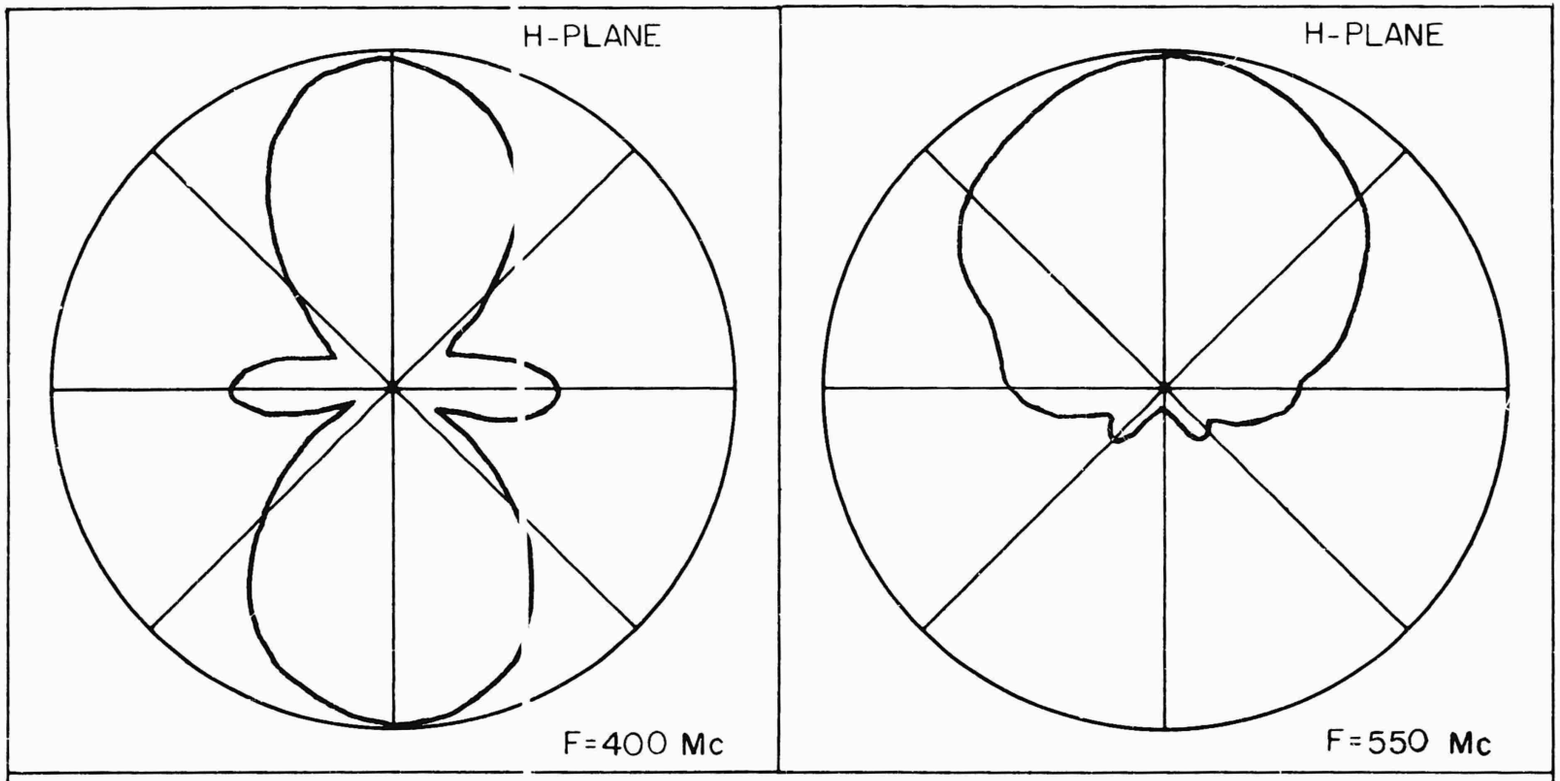

Figure 27. H-plane radiation patterns of uniformly periodic dipole array

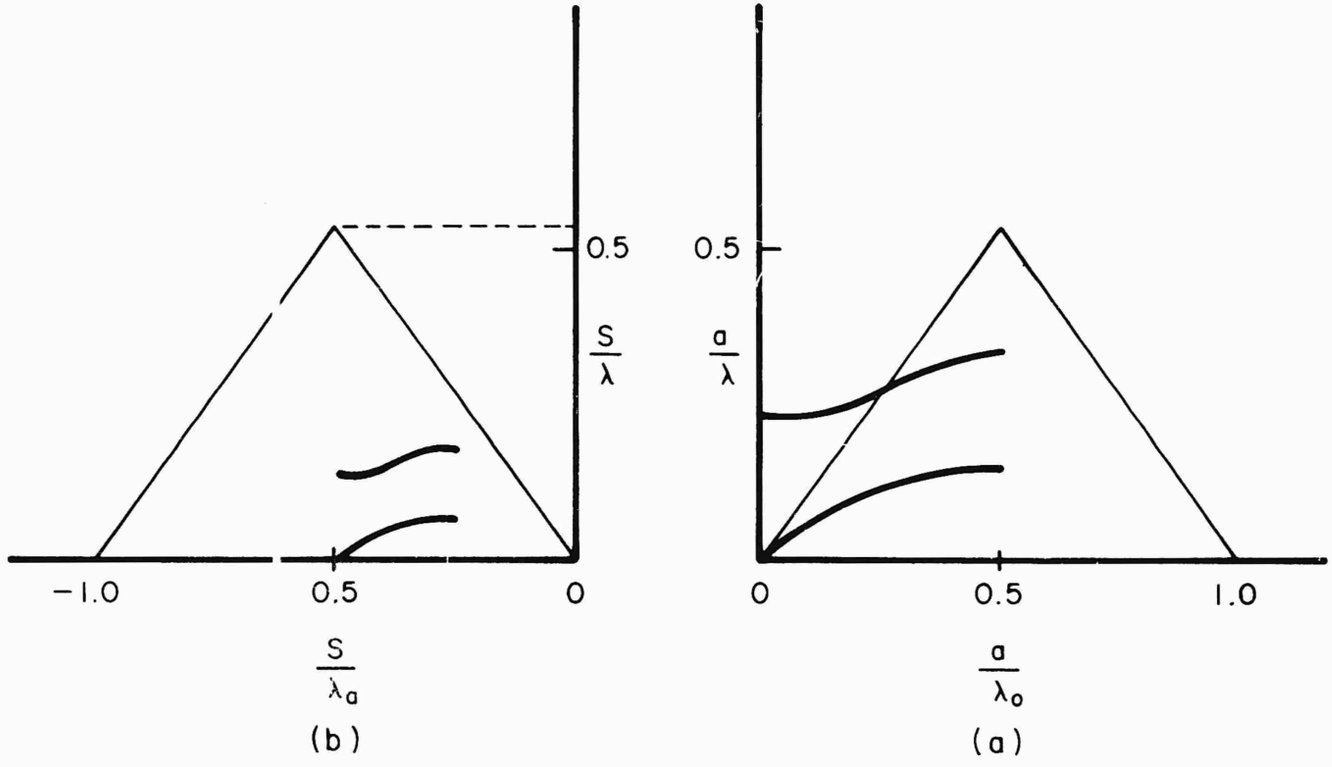

Figure 28. Transformation of measured Brillouin diagram of feeder voltage along periodic dipole array to diagram showing phasing of dipoles

the twist in the feeder adds an addition π radians. To calculate the phase shift between dipoles spaced by $s = a/2$ we can compute a phase constant for the antennas

$$\beta_a s = \frac{\beta_o a}{2} - \pi \tag{13}$$

or, in terms of wavelength λ_a of the wave progressing from dipole to dipole

$$\frac{s}{\lambda_a} = \frac{s}{\lambda_o} - 1/2 \tag{14}$$

Hence the Brillouin diagram for the dipole currents which corresponds to Figure 28a for the feeder currents would appear as shown in Figure 28b. Using the actual data measured on the uniform dipole array from Figure 26 leads to the diagram for the dipole current shown in Figure 29. Note that the phase progression in the dipole currents is opposite to that of the feeder currents. Note also that all points are well within the triangle, removed from the visible range. The radiation is therefore produced by a slow backward wave along the dipoles.

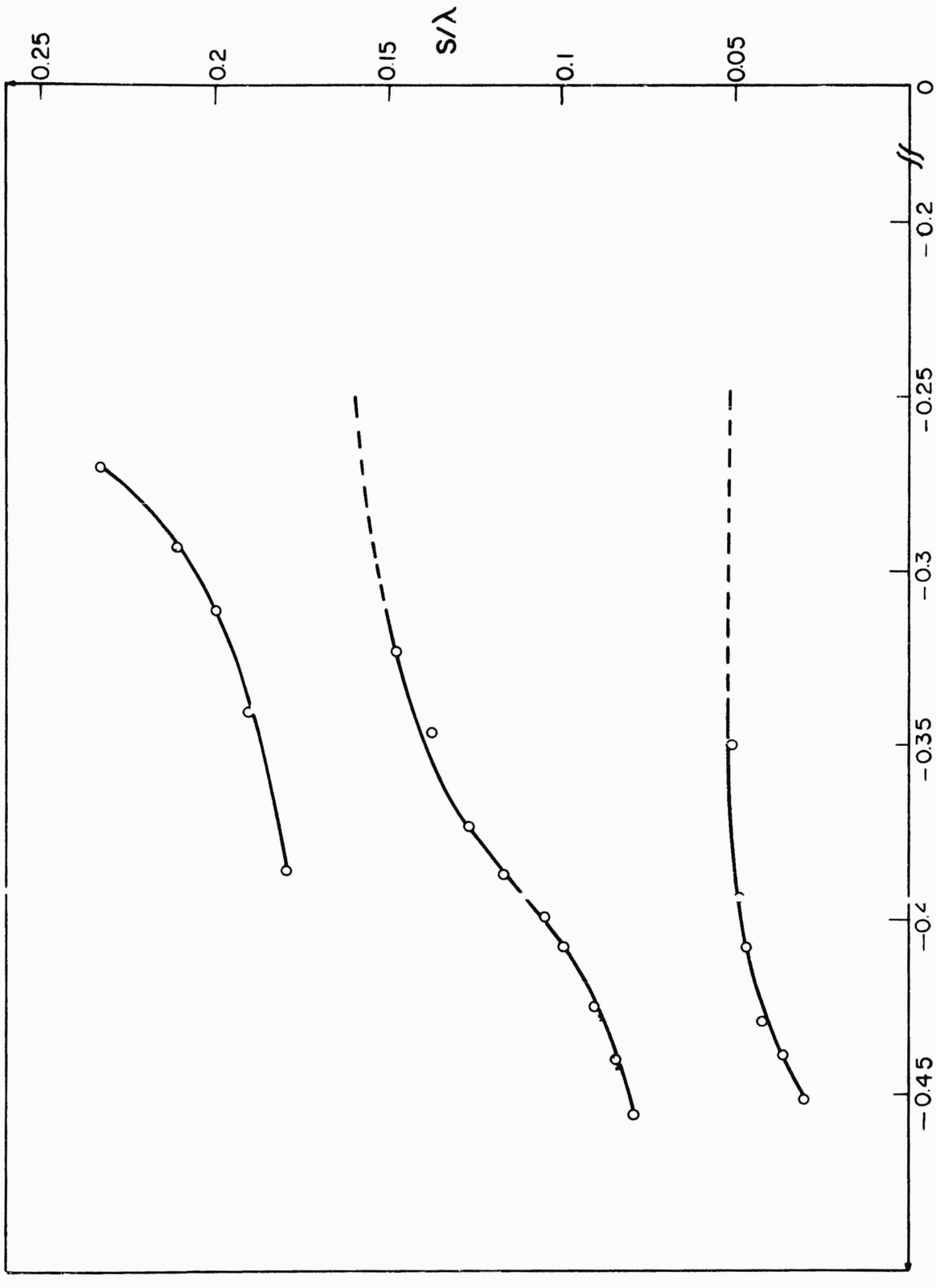

Figure 29. Brillouin diagram for dipole currents

6. CONCLUSIONS

The treatment of the various periodic structures described in this report has been made suggestive and descriptive to illustrate the underlying principle. Detailed studies of most of the structures described here will be the subject of technical reports to follow. Although the relation between periodic structures and log-periodic structures has been emphasized here, the usefulness of the periodic antenna itself should not be overlooked. The periodic antenna has useful properties not shared with log-periodic antennas. Among the notable properties of periodic antennas are the frequency-scanning capability of some of these structures and the absence of sidelobes in the backfire mode. The Brillouin diagram has long been used as a tool in studying and explaining the performance of the closed periodic structures. Here an extension is made to open structures and an interpretation of the diagram for antennas is given. The backfire property is required of the periodic structure to allow tapering to a successful log-periodic antenna.

As our knowledge of these antennas increases it should be possible to satisfy most antenna specifications as to polarization, gain and bandwidth. For example, a gain equivalent to the gain of a linear array of dipoles with Hansen-Woodyard excess phase shift has been obtained with a backfire bifilar helical antenna with a pitch angle of 45 degrees. Needless to say, this antenna has a very narrow bandwidth for this gain. However, gains of this order should be obtainable with the log-periodic version of this antenna if an extremely slow rate of taper were used. In this way, high gain and large bandwidth antennas could be built, but at the expense of very large structures. Where the gain requirements are more moderate a given bandwidth can be achieved with much smaller structures such as the log-spiral of more conventional dimensions[3].

There are many advantages to the viewpoint of periodic structures in antenna design, particularly when the number of elements is large. Treating each element separately in such a case becomes vastly complicated because of the large number of mutual impedances needed to describe the system adequately. From the point of view of periodic structures, the coupling between elements is incorporated in the theory of the infinite structure. This allows the designer to reckon by the forest instead of by the tree.

REFERENCES

1. D E. Isbell, "Non-Planar Logarithmically Periodic Antenna Structures," Tech. Report No. 30, Contract No. AF33(616)-3220, Antenna Laboratory, University of Illinois, Urbana, Illinois.

2. R H. DuHamel and F. R. Ore, "Logarithmically Periodic Antenna Designs," 1958 IRE National Convention Record, pt. 1, p. 139.

3. J. D. Dyson, "The Unidirectional Equiangular Spiral Antenna," IRE Trans., Vol. AP-7, No. 4, p. 329, October, 1959, also Tech. Report No. 33, Contract No. AF33(616)-3220, Antenna Laboratory, University of Illinois, Urbana, Illinois, July, 1958

4. J. K. Shimizu, E. M. Jones, and R. C. Honey, "A Sinuous Flush-Mounted Frequency-Independent Antenna," Scientific Report No. 3, Contract AF19(604)-3502, Stanford Research Institute, Oct. 1959.

5. P. E. Mayes and R L. Carrel, "High Gain Log-Periodic Antennas," Proc. Tenth Symp. USAF Antenna Res. and Dev. Prog., University of Illinois, Allerton Park, Monticello, Illinois, Oct. 1960.

6. J. W. Carr, "Some Variations in Log-Periodic Antenna Structures," IRE Trans. AP-9, p. 229, March 1961.

7. J. W Greiser and P. E. Mayes, "Vertically Polarized Log-Periodic Zig Zag Antennas," Proc National Electronics Conference, Vol. 17, 1961, pp. 193-204.

8. D. E. Isbell, "Log-Periodic Dipole Arrays," IRE Transactions on Antennas and Propagation, Vol AP-8, No. 3, May, 1960, pp. 260-267. Also Tech. Report No. 39, Contract No. AF33(616)-6079, Antenna Laboratory, University of Illinois, Urbana, Illinois, June, 1959.

9. R. L. Carrel, "Analysis and Design of Log-Periodic Dipole Antennas," Convention Record, 1961, IRE International Convention, March, 1961. Also Tech. Report No. 52, Contract No. AF33(616)-6079, Antenna Laboratory, University of Illinois, Oct. 1, 1961.

10. P. E. Mayes and R. L. Carrel," Log-Periodic Resonant-V Arrays," Tech. Report No. 47, Contract No. AF33(616)-6079, Antenna Laboratory, University of Illinois, Urbana, Illinois, July 15, 1960.

ANTENNA LABORATORY

TECHNICAL REPORTS AND MEMORANDA ISSUED

Contract AF33(616)-310

"Synthesis of Aperture Antennas," Technical Report No. 1, C.T.A. Johnk, October, 1954.*

"A Synthesis Method for Broad-band Antenna Impedance Matching Networks," Technical Report No. 2, Nicholas Yaru, 1 February 1955.* AD 61049.

"The Assymmetrically Excited Spherical Antenna," Technical Report No. 3, Robert C. Hansen, 30 April 1955.*

"Analysis of an Airborne Homing System," Technical Report No. 4, Paul E. Mayes, 1 June 1955 (CONFIDENTIAL).

"Coupling of Antenna Elements to a Circular Surface Waveguide," Technical Report No. 5, H. E. King and R. H. DuHamel, 30 June 1955.*

"Axially Excited Surface Wave Antennas," Technical Report No. 7, D. E. Royal, 10 October 1955.*

"Homing Antennas for the F-86F Aircraft (450-2500 mc)," Technical Report No. 8, P. E. Mayes, R. F. Hyneman, and R. C. Becker, 20 February 1957, (CONFIDENTIAL).

"Ground Screen Pattern Range," Technical Memorandum No. 1, Roger R. Trapp, 10 July 1955.*

Contract AF33(616)-3220

"Effective Permeability of Spheroidal Shells," Technical Report No. 9, E. J. Scott and R. H. DuHamel, 16 April 1956.

"An Analytical Study of Spaced Loop ADF Antenna Systems," Technical Report No. 10, D. G. Berry and J. B. Kreer, 10 May 1956. AD 98615.

"A Technique for Controlling the Radiation from Dielectric Rod Waveguides," Technical Report No. 11, J. W. Duncan and R. H. DuHamel, 15 July 1956.*

"Direction Characteristics of a U-Shaped Slot Antenna," Technical Report No. 12, Richard C. Becker, 30 September 1956.**

"Impedance of Ferrite Loop Antennas," Technical Report No. 13, V. H. Rumsey and W. L. Weeks, 15 October 1956. AD 119780.

"Closely Spaced Transverse Slots in Rectangular Waveguide," Technical Report No. 14, Richard F. Hyneman, 20 December 1956.

"Distributed Coupling to Surface Wave Antennas," Technical Report No. 15, Ralph Richard Hodges, Jr., 5 January 1957.

"The Characteristic Impedance of the Fin Antenna of Infinite Length," Technical Report No. 16, Robert L. Carrel, 15 January 1957.*

"On the Estimation of Ferrite Loop Antenna Impedance," Technical Report No. 17, Walter L. Weeks, 10 April 1957.* AD 143989.

"A Note Concerning a Mechanical Scanning System for a Flush Mounted Line Source Antenna," Technical Report No. 18, Walter L. Weeks, 20 April 1957.

"Broadband Logarithmically Periodic Antenna Structures," Technical Report No. 19, R. H. DuHamel and D. E. Isbell, 1 May 1957. AD 140734

"Frequency Independent Antennas," Technical Report No. 20, V. H. Rumsey, 25 October 1957.

"The Equiangular Spiral Antenna," Technical Report No. 21, J. D. Dyson, 15 September 1957. AD 145019.

"Experimental Investigation of the Conical Spiral Antenna," Technical Report No. 22, R. L. Carrel, 25 May 1957.** AD 144021

"Coupling between a Parallel Plate Waveguide and a Surface Waveguide," Technical Report No. 23, E. J. Scott, 10 August 1957.

"Launching Efficiency of Wires and Slots for a Dielectric Rod Waveguide," Technical Report No. 24, J. W. Duncan and R. H. DuHamel, August 1957.

"The Characteristic Impedance of an Infinite Biconical Antenna of Arbitrary Cross Section," Technical Report No. 25, Robert L. Carrel, August 1957.

"Cavity-Backed Slot Antennas," Technical Report No. 26, R. J. Tector, 30 October 1957.

"Coupled Waveguide Excitation of Traveling Wave Slot Antennas," Technical Report No. 27, W. L. Weeks, 1 December 1957.

"Phase Velocities in Rectangular Waveguide Partially Filled with Dielectric," Technical Report No. 28, W. L. Weeks, 20 December 1957.

"Measuring the Capacitance per Unit Length of Biconical Structures of Arbitrary Cross Section," Technical Report No. 29, J. D. Dyson, 10 January 1958.

"Non-Planar Logarithmically Periodic Antenna Structure," Technical Report No. 30, D. E. Isbell, 20 February 1958. AD 156203.

"Electromagnetic Fields in Rectangular Slots," Technical Report No. 31, N. J. Kuhn and P. E. Mast, 10 March 1958.

"The Efficiency of Excitation of a Surface Wave on a Dielectric Cylinder," Technical Report No. 32, J. W. Duncan, 25 May 1958.

"A Unidirectional Equiangular Spiral Antenna," Technical Report No. 33, J. D. Dyson, 10 July 1958. AD 201138

"Dielectric Coated Spheroidal Radiators," Technical Report No. 34, W. L. Weeks, 12 September 1958. AD 204547

"A Theoretical Study of the Equiangular Spiral Antenna," Technical Report No. 35, P. E. Mast, 12 September 1958. AD 204548.

Contract AF33(616)-6079

"Use of Coupled Waveguides in a Traveling Wave Scanning Antenna," Technical Report No. 36, R. H. MacPhie, 30 April 1959. AD 215558

"On the Solution of a Class of Wiener-Hopf Integral Equations in Finite and Infinite Ranges," Technical Report No. 37, Raj Mittra, 15 May 1959.

"Prolate Spheroidal Wave Functions for Electromagnetic Theory," Technical Report No. 38, W. L. Weeks, 5 June 1959.

"Log Periodic Dipole Arrays," Technical Report No. 39, D. E. Isbell, 1 June 1959. AD 220651

"A Study of the Coma-Corrected Zoned Mirror by Diffraction Theory," Technical Report No. 40, S. Dasgupta and Y. T. Lo, 17 July 1959.

"The Radiation Pattern of a Dipole on a Finite Dielectric Sheet," Technical Report No. 41, K. G. Balmain, 1 August 1959.

"The Finite Range Wiener-Hopf Integral Equation and a Boundary Value Problem in a Waveguide," Technical Report No. 42, Raj Mittra, 1 October 1959.

"Impedance Properties of Complementary Multiterminal Planar Structures," Technical Report No. 43, G. A. Deschamps, 11 November 1959.

"On the Synthesis of Strip Sources," Technical Report No. 44, Raj Mittra, 4 December 1959.

"Numerical Analysis of the Eigenvalue Problem of Waves in Cylindrical Waveguides," Technical Report No. 45, C. H. Tang and Y. T. Lo, 11 March 1960.

"New Circularly Polarized Frequency Independent Antennas with Conical Beam or Omnidirectional Patterns," Technical Report No. 46, J. D. Dyson and P. E. Mayes, 20 June 1960. AD 241321

"Logarithmically Periodic Resonant-V Arrays," Technical Report No. 47, P. E. Mayes and R. L. Carrel, 15 July 1960. AD 246302

"A Study of Chromatic Aberration of a Coma-Corrected Zoned Mirror," Technical Report No. 48, Y. T. Lo, June 1960.

"Evaluation of Cross-Correlation Methods in the Utilization of Antenna Systems," Technical Report No. 49, R. H. MacPhie, 25 January 1961.

"Synthesis of Antenna Products Patterns Obtained from a Single Array," Technical Report No. 50, R. H. MacPhie, 25 January 1961.

"On the Solution of a Class of Dual Integral Equations," Technical Report No. 51, R. Mittra, 1 October 1961. AD 264557

"Analysis and Design of the Log-Periodic Dipole Antenna," Technical Report No. 52, Robert L. Carrel, 1 October 1961.* AD 264558

"A Study of the Non-Uniform Convergence of the Inverse of a Doubly-Infinite Matrix Associated with a Boundary Value Problem in a Waveguide," Technical Report No. 53, R. Mittra, 1 October 1961. AD 264556

---

*Copies available for a three-week loan period.

**Copies no longer available.

AF33(657)-8460

DISTRIBUTION LIST

One copy each unless otherwise indicated

Armed Services Technical Information Agency
Attn: TIP-DR
Arlington Hall Station
Arlington 12, Virginia (10 copies)

Aeronuatical Systems Division
Attn: (ASRNCF-3)
Wright-Patterson Air Force Base
Ohio (3 copies)

Aeronautical Systems Division
Attn: ASDSED, Mr. Mulligan
Wright-Patterson Air Force Base
Ohio

Aeronautical Systems Division
Attn: AFCIN-4B1A
Wright-Patterson Air Force Base
Ohio

Air Force Cambridge Research Laboratory
Attn: CRRD
Laurence G. Hanscom Field
Bedford, Massachusetts

Commander
Air Force Missile Test Center
Patrick Air Force Base
Florida

Commander
Air Force Missile Development Center
Attn: Technical Library
Holloman Air Force Base
New Mexico

Air Force Ballistic Missile Division
Attn: Technical Library, Air Force Unit Post Office
Los Angeles, California

Director
Ballistics Research Laboratory
Attn: Ballistics Measurement Lab.
Aberdeen Proving Ground, Maryland

National Aeronautics & Space Adm.
Attn: Librarian
Langley Field, Virginia

Rome Air Development Center
Attn: RCLTM
Griffiss Air Force Base
New York

Research & Development Command
Hq. USAF (ARDRD-RE)
Washington 25, D. C.

Office of Chief Signal Officer
Engineering & Technical Division
Attn: SIGNET-5
Washington 25, D. C.

Commander
U. S. Army White Sands Signal Agency
Attn: SIGWS-FC-02
White Sands. New Mexico

Director
Surveillance Department
Evans Area
Attn: Technical Document Center
Belman, New Jersey

Commander
U. S. Naval Air Test Center
Attn: WST-54, Antenna Section
Patuxent River, Maryland

Material Laboratory, Code 932
New York Naval Shipyard
Brooklyn 1, New York

Commanding Officer
Diamond Ordnance Fuse Laboratories
Attn: 240
Washington 25, D. C.

Director
U. S. Navy Electronics Laboratory
Attn: Library
San Diego 52, California

Adams-Russell Company
200 Sixth Street
Attn: Library (Antenna Section)
Cambridge, Massachusetts

Aero Geo Astro
Attn: Security Officer
1200 Duke Street
Alexandria, Virginia

NASA Goddard Space Flight Center
Attn: Antenna Section, Code 523
Greenbelt, Maryland

Airborne Instruments Labs., Inc.
Attn: Librarian (Antenna Section)
Walt Whitman Road
Melville, L. I., New York

American Electronic Labs
Box 552 (Antenna Section)
Lansdale, Pennsylvania

Andrew Alfred Consulting Engineers
Attn: Librarian (Antenna Section)
299 Atlantic Ave
Boston 10, Massachusetts

Ampheol-Borg Electronic Corporation
Attn: Librarian (Antenna Section)
2801 S. 25th Avenue
Broadview, Illinois

Bell Aircraft Corporation
Attn: Technical Library
(Antenna Section)
Buffalo 5, New York

Bendix Radio Division of
Bendix Aviation Corporation
Attn: Technical Library
(For Dept. 462-4)
Baltimore 4, Maryland

Boeing Airplane Company
Aero Space Division
Attn: Technical Library
M/F Antenna & Radomes Unit
Seattle, Washington

Boeing Airplane Company
Attn: Technical Library
M/F Antenna Systems Staff Unit
Wichita, Kansas

Chance Vought Aircraft Inc.
THRU: BU AER Representative
Attn: Technical Library
M/F Antenna Section
P. O. Box 5907
Ballas 22, Texas

Collins Radio Company
Attn: Technical Library (Antenna
Section)
Dallas, Texas

Convair
Ft. Worth Division
Attn: Technical Library (Antenna
Section)
Grants Lane
Fort Worth, Texas

Convair
Attn: Technical Library (Antenna
Section)
P. O. Box 1050
San Diego 12, California

Dalmo Victor Company
Attn: Technical Library (Antenna
Section)
1515 Industrial Way
Belmont, California

Dorne & Margolin, Inc.
Attn: Technical Library (Antenna
Section)
30 Sylvester Street
Westbury, L. I., New York

Dynatronics Inc.
Attn: Technical Library (Antenna
Section)
Orlando, Florida

Electronic Communications, Inc.
Research Division
Attn: Technical Library
1830 York Road
Timonium, Maryland

Fairchild Engine & Airplane Corporation
Fairchild Aircraft & Missiles Division
Attn: Technical Library (Antenna Section)
Hagerstown 10, Maryland

Georgia Institute of Technology
Engineering Experiment Station
Attn: Technical Library
M/F Electronics Division
Atlanta 13, Georgia

General Electric Company
Electronics Laboratory
Attn: Technical Library
Electronics Park
Syracuse, New York

General Electronic Labs., Inc.
Attn: Technical Library (Antenna Section)
18 Ames Street
Cambridge 42, Massachusetts

General Precision Lab., Division of General Precision Inc.
Attn: Technical Library (Antenna Section)
63 Bedford Road
Pleasantville, New York

Goodyear Aircraft Corporation
Attn: Technical Library
M/F Dept. 474
1210 Massilon Road
Akron 15, Ohio

Granger Associates
Attn: Technical Library (Antenna Section)
974 Commercial Street
Palo Alto, California

Grumman Aircraft Engineering Corp.
Attn: Technical Library
M/F Avionics Engineering
Bethpage, New York

The Hallicrafters Company
Attn: Technical Library (Antenna Section)
4401 W. Fifth Avenue
Chicago 24, Illinois

Hoffman Laboratories Inc.
Attn: Technical Library (Antenna Section)
Los Angeles 7, California

John Hopkins University
Applied Physics Laboratory
8621 Georgia Avenue
Silver Springs, Maryland

Hughes Aircraft Corporation
Attn: Technical Library (Antenna Section)
Florence & Teal Street
Culver City, California

ITT Laboratories
Attn: Technical Library (Antenna Section)
500 Washington Avenue
Nutley 10, New Jersey

U. S. Naval Ordnance Lab.
Attn: Technical Library
Corona, California

Lincoln Laboratories
Massachusetts Institute of Technology
Attn: Document Room
P. O. Box 73
Lexington 73, Massachusetts

Litton Industries
Attn: Technical Library (Antenna Section)
4900 Calvert Road
College Park, Maryland

Lockheed Missile & Space Division
Attn: Technical Library (M/F Dept-58-40, Plant 1, Bldg. 130)
Sunnyvale, California

The Martin Company
Attn: Technical Library (Antenna Section)
P. O. Box 179
Denver 1, Colorado

The Martin Company
Attn: Technical Library (Antenna Section) Mail No. T-38
Baltimore 3, Maryland

The Martin Company
Attn: Technical Library (M/F Microwave Laboratory)
Box 5837
Orlando, Florida

W. L. Maxson Corporation
Attn: Technical Library (Antenna Section)
460 West 34th Street
New York 1, New York

McDonnell Aircraft Corporation
Attn: Technical Library (Antenna Section)
Box 516
St. Louis 66, Missouri

Melpar, Inc.
Attn: Technical Library (Antenna Section)
3000 Arlington Blvd.
Falls Church, Virginia

University of Michigan
Radiation Laboratory
Willow Run
201 Catherine Street
Ann Arbor, Michigan

Mitre Corporation
Attn: Technical Library (M/F Electronic Warfare Dept. D-21)
Middlesex Turnpike
Bedford, Massachusetts

North American Aviation Inc.
Attn: Technical Library (M/F Engineering Dept.)
4300 E. Fifth Avenue
Columbus 16, Ohio

North American Aviation Inc.
Attn: Technical Library (M/F Dept. 56)
International Airport
Los Angeles, California

Northrop Corporation
NORAIR Division
1001 East Broadway
Attn: Technical Information (3924-3)
Hawthorne, California

Ohio State University Research Foundation
Attn: Technical Library (M/F Antenna Laboratory)
1314 Kinnear Road
Columbus 12, Ohio

Philco Corporation
Government & Industrial Division
Attn: Technical Library (M/F Antenna Section)
4700 Wissachickon Avenue
Philadelphia 44, Pennsylvania

Westinghouse Electric Corporation
Air Arms Division
Attn: Librarian (Antenna Lab)
P. O. Box 746
Baltimore 3, Maryland

Wheeler Laboratories
Attn: Librarian (Antenna Lab)
Box 561
Smithtown, New York

Electrical Engineering Research Laboratory
University of Texas
Box 8026, Univ. Station
Austin, Texas

University of Michigan Research Institute
Electronic Defense Group
Attn: Dr. J. A. M. Lyons
Ann Arbor, Michigan

Radio Corporation of America
RCA Laboratories Division
Attn: Technical Library
(M/F Antenna Section)
Princeton, New Jersey

Radiation, Inc.
Attn: Technical Library (M/F)
Antenna Section
Drawer 37
Melbourne, Florida

Radioplane Company
Attn: Librarian (M/F Aerospace Lab)
8000 Woodly Avenue
Van Nuys, California

Ramo-Wooldridge Corporation
Attn: Librarian (Antenna Lab)
Conoga Park, California

Rand Corporation
Attn: Librarian (Antenna Lab)
1700 Main Street
Santa Monica, California

Rantec Corporation
Attn: Librarian (Antenna Lab)
23999 Ventura Blvd.
Calabasas, California

Raytheon Corporation
Equipment Division
Library - J. Portsch
P. O. Box 520
Waltham 54, Massachusetts

Republic Aviation Corporation
Applied Research & Development
Division
Attn: Librarian (Antenna Lab)
Farmingdale, New York

Sanders Associates
Attn: Librarian (Antenna Lab)
95 Canal Street
Nashua, New Hampshire

Southwest Research Institute
Attn: Librarian (Antenna Lab)
8500 Culebra Road
San Antonio, Texas

H. R. B. Singer Corporation
Attn: Librarian (Antenna Lab)
State College, Pennsylvania

Sperry Microwave Electronics Company
Attn: Librarian (Antenna Lab)
P. O. Box 1828
Clearwater, Florida

Sperry Gyroscope Company
Attn: Librarian (Antenna Lab)
Great Neck, L. I., New York

Stanford Electronic Laboratory
Attn: Librarian (Antenna Lab)
Stanford, California

Stanford Research Institute
Attn: Librarian (Antenna Lab)
Menlo Park, California

Sylvania Electronic System
Attn: Librarian (M/F Antenna &
Microwave Lab)
100 First Street
Waltham 54, Massachusetts

Sylvania Electronic System
Attn: Librarian (Antenna Lab)
P. O. Box 188
Mountain View, California

Technical Research Group
Attn: Librarian (Antenna Section)
2 Aerial Way
Syosset, New York

Ling Temco Aircraft Corporation
Temco Aircraft Division
Attn: Librarian (Antenna Lab)
Garland, Texas

Texas Instruments, Inc.
Attn: Librarian (Antenna Lab)
6000 Lemmon Ave.
Dallas 9, Texas

A. S. Thomas, Inc.
Attn: Librarian (Antenna Lab)
355 Providence Highway
Westwood, Massachusetts

New Mexico State University
Head Antenna Department
Physical Science Laboratory
University Park, New Mexico

Bell Telephone Laboratories, Inc.
Whippany Laboratory
Whippany, New Jersey
Attn: Technical Reports Librarian
Room 2A-165

Robert C. Hansen
Aerospace Corporation
Box 95085
Los Angeles 45, California

Dr. Richard C. Becker
10829 Berkshire
Westchester, Illinois

Dr. W. M. Hall
Raytheon Company
Surface Radar and Navigation
Operations
Boston Post Road
Wayland, Massachusetts

Mr. Dwight Isbell
1422 11th West
Seattle 99, Washington

Dr. Robert L. Carrel
Collins Radio Corporation
Antenna Section
Dallas, Texas

Dr. A. K. Chatterjee
Vice Principal & Head of the Department
of Research
Birla Institute of Technology
P. O. Mesra
District-Ranchi (Bihar) India

Aeronautical Systems Division
Attn: ASAD - Library
Wright-Patterson Air Force Base
Ohio

National Bureau of Standards
Department of Commerce
Attn: Dr A. G. McNish
Washington 25, D. C

Aeronautic Division
Ford Motor Company
Ford Road
Attn: Mr. J. M Black

University of Dayton
Research Institute
Attn: Professor Douglas Hanneman
300 College Park

Technische Hochschule
Attn: H. H. Meinke
Menick, Germany

NASA Goddard Space Flight Center
Attn: Antenna Branch,
Mr. Lantz
Greenbelt, Maryland

Professor A. A. Abner
Polytechnic Institute of Brooklyn
Microwave Research Institute
55 Johnson Street
Brooklyn 1, New York

U. S. Naval Ordnance Laboratory
Attn: Technical Library
Corona, California

Avco Corporation
Research and Advanced Development Division
Attn: Research Library/T.A. Rupprecht
201 Lowell Street
Wilmington, Mass.

Raytheon Company
Missile and Space Division
Attn: Research Library
Bedford, Mass.

American Systems Incorporated
Attn: Technical Library/Antenna Section
1625 East 126th Street
Hawthorne, California

National Research Council
Attn: Microwave Section
Ottawa 2, Canada

Sichak Associates
Attn: W Sichak
518 Franklin Avenue
Nutley, New Jersey

W. T. Patton
2208 New Abany Road
Cinn. Township
Riverton Post Office
New Jersey

Radio Corporation of America
Missile and Service Radar Division
Attn: Manager
Antenna Engineering Skill Center
Moorestown, New Jersey

Commander
Air Force Systems Command
Aeronautical Systems Division
Wright-Patterson Air Force Base
Ohio
Attn: ASNCSO

Commander
Air Force Systems Command
Aeronautical Systems Division
Wright-Patterson Air Force Base
Ohio
Attn: ASNPOT, Mr. Finocharo